

Structural diversity of building-blocks in coordination framework synthesis—combining $M(NO_3)_2$ junctions and bipyridyl ligands

Sarah A. Barnett, Neil R. Champness*

School of Chemistry, The University of Nottingham, University Park, Nottingham NG7 2RD, UK

Received 7 February 2003; accepted 17 June 2003

Contents

Abstract	146
1. Introduction to coordination frameworks and the building-block methodology	146
1.1. Transition metal dinitrate connecting nodes	146
2. $M(NO_3)_2$ bis-pyridyl structures—1D polymer architectures	148
2.1. $M(NO_3)_2$ bis-pyridyl structures without nitrate bridging	149
2.2. $M(NO_3)_2$ bis-pyridyl structures with nitrate bridging	150
3. $M(NO_3)_2$ tris-pyridyl structures—T-shaped connecting nodes	152
3.1. Potential architectures using T-shaped connecting nodes	153
3.2. Coordination frameworks observed with T-shaped connecting nodes	153
3.2.1. Cobalt (II) nitrate architectures	154
3.2.2. Nickel (II) nitrate architectures	158
3.2.3. Zinc(II) nitrate architectures	158
3.2.4. Cadmium (II) nitrate architectures	158
3.3. Summary of observed architectures with T-shaped $M(NO_3)_2$ connecting nodes	160
4. $M(NO_3)_2$ tetrakis-pyridyl structures	160
4.1. Tetrakis-pyridyl double-bridged 1D chain structures	160
4.2. Tetrakis-pyridyl (4,4)-grid 2D frameworks	161
4.2.1. Non-interpenetrated (4,4) 2D frameworks	162
4.2.2. Interpenetrated (4,4) 2D frameworks	162
4.2.3. Other 2D tetrakis-pyridyl frameworks	164
4.3. Tetrakis-pyridyl 3D architectures	165
5. Architectures containing more than one type of $M(NO_3)_2$ node	166
6. Conclusions, structural reliability and future developments	167
Acknowledgements	167
References	167

Abbreviations: 4,4'-bipy, 4,4'-bipyridine; 2,4'-bipy, 2,4'-bipyridine; b2psmb, 1,4-bis(2-pyridylsulfenylmethyl)benzene; bpsmb, 1,4-bis(4-pyridylsulfenylmethyl)benzene; bpobp, 4,4'-bis(4-pyridylmethoxy)biphenyl; bpmob, 4,4'-bis(4-pyridylmethoxy)benzene; bpoph, 1,4-bis(4-pyridyl)benzene; bpanth, 9,10-bis(4-pyridyl)anthracene; bptri, 2,4-bis(4-pyridyl)-1,3,5-triazine; bpbdiyne, 1,4-bis-(4-pyridyl)butadiyne; bpmeth, 1,1-bis(4-pyridyl)methane; bpeth, 1,2-bis(4-pyridyl)ethane; bpro, 1,3-bis(4-pyridyl)propane; bpbut, 1,4-bis(4-pyridyl)butane; bpent, 1,5-bis(4-pyridyl)pentane; bphe, 1,6-bis(4-pyridyl)hexane; bpethene, 1,2-bis(4-pyridyl)ethene; bpethyne, 1,2-bis(4-pyridyl)ethyne; b3pethyne, 1,2-bis(3-pyridyl)ethyne; b2pethyne, 1,2-bis(2-pyridyl)ethyne; btp, bis(4-pyridyl)terephthalate; 2,4'-bpoph, 2,4'-(1,4-phenylene)bispyridine; 2,4'-bpacph, 2,4'-(4-ethynylphenyl)bipyridyl; 2,4'-bpophac, 2,4'-(2-ethynylphenyl)bipyridyl; bpdahd, 2,5-bis(4-pyridyl)-3,4-diaza-2,4-hexadiene; b3pdahd, 2,5-bis(3-pyridyl)-3,4-diaza-2,4-hexadiene; bpdabd, 1,2-bis(4-pyridyl)-2,3-diaza-1,3-butadiene; b3pdabd, 1,2-bis(3-pyridyl)-2,3-diaza-1,3-butadiene; b3ptz, 1,4-bis(3-pyridyl)-2,3,5,6-tetrazine; bptz, 1,4-bis(4-pyridyl)-2,3,5,6-tetrazine; bpm, 1,4-bis(4-pyridyl)methyl-benzene; bpmfb, 1,4-bis(4-pyridyl)methyl-2,3,5,6-tetrafluorobenzene; bpsfb, 2,3,5,6-tetrafluoro-1,4-bis(4-pyridyl-sulfenyl)benzene; bpob, 1,4-bis(4-pyridoxy)benzene; azpy, *trans*-4,4'-azobis(4-pyridine); 2,4'-bpma, *N*-(2-pyridyl)-(4-pyridyl)methanamine; bpmom, 1,5-bis(4-pyridylmethoxy)naphthalene; bpobp, 4,4'-bis(4-pyridyl)biphenyl; bpmfbp, 1,1'-bis(4-pyridylmethyl)[2,2',3,3',5,5',6,6'-octafluorobiphenyl]; bpmfnap, 2,6-bis(4-pyridylmethyl)-1,3,4,5,7,8-hexafluoronaphthalene; bpbe, 1,2-bis[2-(4-pyridyl)ethyl]benzene

* Corresponding author.

E-mail address: neil.champness@nottingham.ac.uk (N.R. Champness).

Abstract

The construction of coordination framework polymers using transition metal complexes of bridging bidentate ligands is a high profile area of chemistry that has received considerable attention over recent years. This article will review the complexity of the area of coordination frameworks which aims to use $M(\text{NO}_3)_2$ ($M = \text{Co}, \text{Ni}, \text{Cu}, \text{Zn}, \text{Cd}$) building-blocks as junctions in combination with bipyridyl-based ligands. The variety of network topologies and structural motifs that have been constructed thus far will be outlined illustrating the range of coordination environments that are adopted by the $M(\text{NO}_3)_2$ nodes and the influence that this has on the coordination framework topology.

© 2003 Elsevier B.V. All rights reserved.

Keywords: Crystal engineering; Coordination framework; Nitrate; Cobalt; Nickel; Copper; Zinc; Cadmium; Topology

1. Introduction to coordination frameworks and the building-block methodology

The development of inorganic supramolecular networks and coordination polymers is an area of chemistry that is extremely topical [1–3]. This is due to fundamental interest in self-assembly processes [4], supramolecular chemistry [5] and perhaps, most significantly, crystal engineering [6]. The rational design of 3D molecular architectures is also of great importance when synthesising new materials as the arrangement of the components within a material will affect its properties. Some success has been achieved in the synthesis of coordination framework materials with solvent-inclusion [7–10] or gas adsorption [10–12] characteristics or, with electronic [13] or non-linear optical properties [14].

The coordination polymers produced have been shown to form a wide range of interesting network topologies using a building-block methodology [15]. The framework structure is primarily dependent upon the coordination preferences of the metal-unit and the functionality of the ligand. Thus, in combination with a linear bridging ligand, such as a 4,4'-bipyridyl derivative, a linear metal centre will afford a chain structure [16], and a tetrahedral metal node a diamondoid array [17]. Other metal node geometries are typically topologically variable and can lead to more complex arrays. For example, a square-planar metal centre may afford a 2D (4,4) grid structure or 3D structures with $\text{Cd}(\text{SO}_4)$ [18] or NbO [19] topology. In the case of the more flexible systems the role of more subtle factors, such as templating species, can become more important.

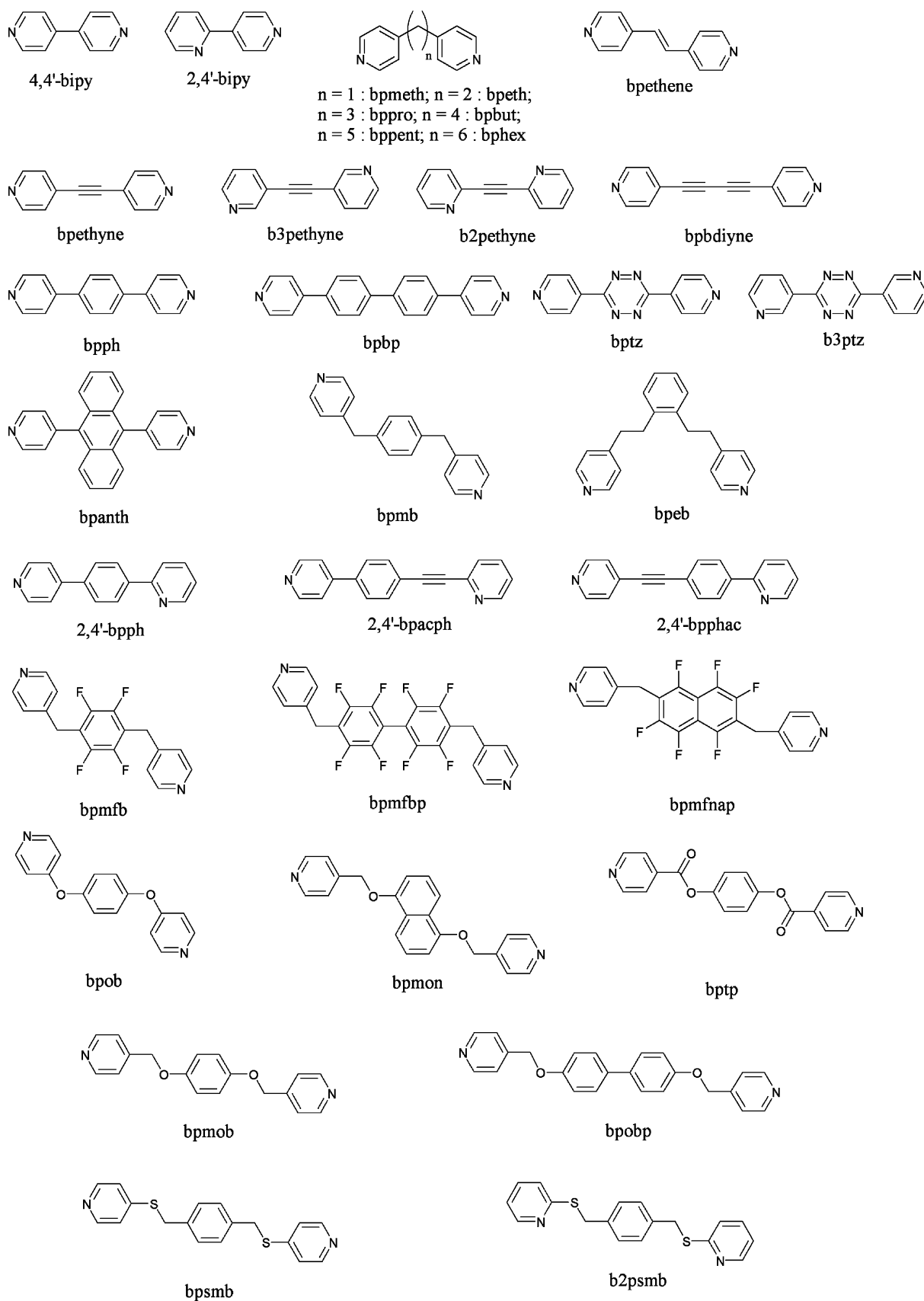
In particular the counter-anion has a significant role to play in influencing the network structure, primarily by acting as either a coordinating or non-coordinating building-block. Nitrate is a particularly interesting anion in this respect due to its coordinative flexibility.

1.1. Transition metal dinitrate connecting nodes

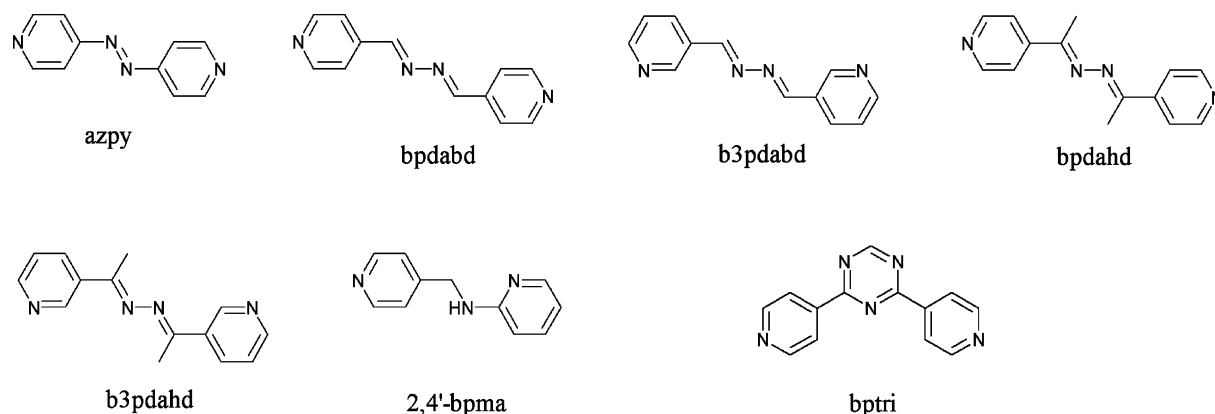
The nitrate anion exhibits many intriguing features when it is used as the anionic building-block in constructing coordination networks. Commonly, when the nitrate anion is present in such a network, an entirely different structural motif or topology is observed when compared to analogous

systems with other counter-anions such as BF_4^- , PF_6^- , Cl^- or SCN^- . This behaviour is caused by the flexible coordinating ability of the nitrate anion. Clearly the nitrate anion does not have to coordinate to the metal centre and this will be the case when in competition with particularly strongly binding ligands for a given metal centre. When the nitrate anion is coordinated its ability to disrupt a metal ions coordination environment varies from weak interactions, through weak monodentate coordination to strong bidentate coordination. It is also possible for the nitrate to bridge metal centres using two, or potentially three, of the oxygen donors to coordinate metal centres. The extent of the metal–nitrate interaction is mostly dependent on the nature of the metal centre in question and the coordinating ability of the other ligands being used for coordination polymer construction. The combination of nitrate anions and pyridyl donor ligands leads to a subtle balance of nitrate vs. pyridyl coordination resulting in interesting anion effects and this is the subject matter of this review.

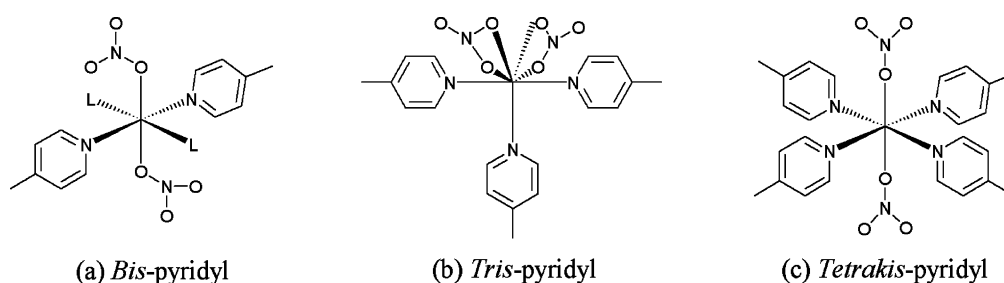
This review will focus on the use of $M(\text{NO}_3)_2$ [$M = \text{Co}(\text{II}), \text{Ni}(\text{II}), \text{Cu}(\text{II}), \text{Zn}(\text{II}), \text{Cd}(\text{II})$] in constructing coordination networks with bipyridyl ligands such as those illustrated in Scheme 1. A number of combinations of nitrate coordination modes have been observed in conjunction with bridging bipyridyl ligands which can lead to different metal:ligand ratios in the coordination polymer products. Hence, the different coordination modes of the nitrate anions as well as bipyridyl functionality leads to a range of different coordination polymer structures in which the number of coordinated pyridyl groups results in the adoption of one of three distinct connecting nodes (Scheme 2). In the case of bis-pyridyl metal coordination environments (Scheme 2a) simple, 1D chains, are formed when only the bipyridyl ligand is involved in polymeric propagation and the remaining coordination sites are occupied by other ligands, such as H_2O (see Section 2). More complex framework structures are observed for either tris- or tetrakis-pyridyl metal coordination environments. Tris-pyridyl metal centres commonly lead to the formation of T-shaped connecting units (Scheme 2b) which are linked via the bridging bipyridyl ligands to afford a family of highly related 1D, 2D and 3D polymeric architectures (see Section 3). Tetrakis-pyridyl metal coordination environments (Scheme 2c) almost uniformly assume



Scheme 1. Ligands referred to in this article with abbreviations.



Scheme 1. (Continued).

Scheme 2. $M(\text{NO}_3)_2$ —pyridyl coordination modes discussed in this review.

trans monodentate nitrate coordination modes and consequently the ligands adopt an equatorial coordination mode. Thus, the $M(\text{NO}_3)_2(\text{py})_4$ node acts as a square-planar junction leading to the formation of frameworks based upon that structural motif, square-grid structures or 3D architectures (see Section 4). Nitrate bridging between metal centres can also be observed and this gives rise to many unusual structures which will be discussed separately. It is important to note that in many instances the M:pyridyl ratio observed in the product coordination framework is independent of the reaction M:pyridyl stoichiometry.

Each of these different coordination polymer metal:ligand ratios will be dealt with in turn and the structures that are observed, described and compared. It is important to note that for a given $M(\text{NO}_3)_2$ and ligand it is possible to observe more than one product with potentially different metal:ligand ratios and different structural architectures. Where this is the case, it will be noted in the text.

2. $M(\text{NO}_3)_2$ bis-pyridyl structures—1D polymer architectures

The formation of bis-pyridyl $M(\text{NO}_3)_2$ coordination polymers instead of frameworks with a higher metal–pyridyl ratio, i.e. tris- or tetrakis-pyridyl systems, is dependent upon two possible factors. The major consideration is the relative binding ability of the pyridyl ligand in comparison to all other possible donors in the reaction process. Thus, the

nitrate anion needs to be considered as a competitive donor as well as coordinating molecules which may be introduced either with the metal salt, for example as a hydrate, or as the reaction solvent (H_2O , MeCN etc.).

The second factor that needs to be considered is whether the product formed is a kinetic product rather than the thermodynamic product from the reaction process. This is a particularly important consideration for coordination frameworks where the insolubility of the polymeric product may favour the isolation of kinetic products.

The formation of 1D $M(\text{NO}_3)_2$ coordination polymers in which only two of the metal coordination sites are occupied by pyridyl groups is relatively rare. This is, presumably, a result of the considerations discussed above, i.e. competitor ligands do not contend with the relatively favourable M–pyridyl bond formation for the metals studied. As the two nitrate anions can occupy a maximum of four coordination sites, both in a bidentate fashion, it is more likely that three pyridyl ligands will be coordinated to the metal centre due to the sterically undemanding nature of the bidentate nitrate. Indeed, tris- and tetrakis-pyridyl coordination polymers are significantly more common than the corresponding bis-pyridyl species, see Sections 3 and 4. Other possible ligands such as H_2O , ROH or RCN rarely offer significant competition as ligands for the later transition metals in comparison to pyridyl groups.

The structures observed fall into two broad categories, those with and those without metal–nitrate bridging which can lead to radically different structures and unusual motifs.

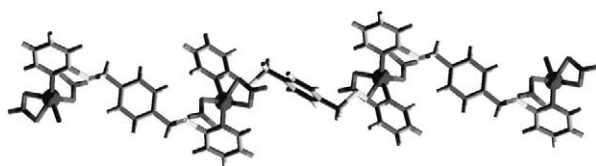


Fig. 1. View of the 1D chains formed by $\{\text{Co}(\text{NO}_3)_2[\text{b2psb}]\}_\infty$ exhibiting bis-pyridyl coordination at the Co(II) centre [20].

Thus, these two different classes of compounds will be dealt with in turn.

2.1. $M(\text{NO}_3)_2$ bis-pyridyl structures without nitrate bridging

Bis-pyridyl $M(\text{NO}_3)_2$ coordination polymers form one of two broad types, chains or discrete metallacycles, depending on the nature of the ligand used. Normally with exodentate pyridyl ligands, such as those related to 4,4'-bipy, chains are observed with the remaining metal coordination sites occupied by the nitrate anion or other ligands such as H_2O .

$\text{Co}(\text{NO}_3)_2$ reacts with 1,4-bis(2-pyridylsulfenylmethyl)benzene (b2psmb) to afford 1D chains, $\{\text{Co}(\text{NO}_3)_2[\text{b2psb}]\}_\infty$ (Fig. 1) [20]. Each Co(II) centre adopts a five-coordinate geometry with a bis-pyridyl arrangement and one monodentate and one bidentate nitrate ligand. The analogous Ni(II) complex is believed to adopt a similar polymeric architecture but with octahedral Ni(II) cations with two bidentate nitrate anions, on the basis of solid-state UV–visible spectroscopy [20]. A similar structural arrangement is adopted by $\{\text{Co}(\text{NO}_3)_2[\text{bpobp}]\}_\infty$ [bpobp = 4,4'-bis(4-pyridylmethoxy)biphenyl] but with a zig-zag chain being isolated due to the *cis* arrangement of the pyridyl ligands at the Co(II) centre [21]. $\{\text{Cu}(\text{NO}_3)_2[\text{bpanth}]\}_\infty$ [bpanth = 9,10-bis(4-pyridyl)anthracene] similarly forms 1D zig zag chains as a result of the *cis*-pyridyl arrangement at the square-planar Cu(II) centre [22].

$\text{Zn}(\text{NO}_3)_2$ reacts with 2,4-bis(4-pyridyl)-1,3,5-triazine (bptri) in either a 1:1 or 2:1 L:M ratio to afford the 1D polymer, $[\text{Zn}(\text{NO}_3)_2(\text{bptri})]_\infty$, which can be isolated as two polymorphs [23]. In both cases the Zn(II) cation is bound by two pyridyl donors from two independent bptri ligands which act as bridges between metal centres thus generating polymeric propagation. The two polymorphs differ in their nitrate binding modes such that in one both nitrate anions coordinate in a bidentate fashion whereas in the other polymorph one nitrate acts in a monodentate and one in a bidentate fashion. The difference between the nitrate binding modes results in a different helical pitch along the 1D polymer from 22.576 Å in the form with two bidentate nitrate anions to 19.029 Å in other polymorph (one monodentate, one bidentate nitrate) (Fig. 2). When either EtOH/ CH_2Cl_2 or $i\text{PrOH}/\text{CH}_2\text{Cl}_2$ solvent mixtures are used as reaction solvents both polymorphs are generated whereas when MeCN/ CH_2Cl_2 is used as the reaction solvent only the bis-bidentate structure is observed.

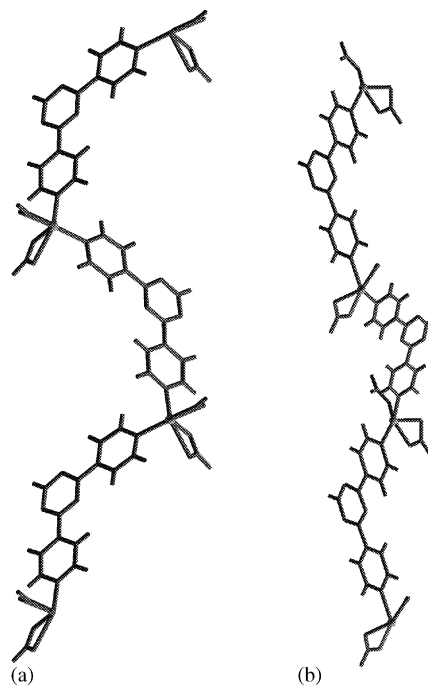


Fig. 2. View of the two polymorphs of the 1D polymers formed by $[\text{Zn}(\text{NO}_3)_2(\text{bptri})]_\infty$, illustrating the bis-bidentate nitrate coordination in (a) and mono and bidentate nitrate coordination in (b) [23].

In contrast, the analogous reactions between bptri and $\text{Cd}(\text{NO}_3)_2$ generates different species reflecting the higher coordination number of this metal centre [23]. The discrete molecular complex $[\text{Cd}(\text{NO}_3)_2(\text{bptri})_2(\text{MeCN})]$ in which both bptri ligands act as terminal donors rather than acting as bridges between metal centres is prepared by reacting a 2:1 L:M ratio in MeCN/ CH_2Cl_2 . Reaction of $\text{Cd}(\text{NO}_3)_2$ with bptri in EtOH/ CH_2Cl_2 affords a 1D coordination polymer $[\text{Cd}(\text{NO}_3)_2(\text{bptri})(\text{EtOH})]_\infty$ in which each Cd(II) cation adopts a bis-pyridyl coordination sphere accompanied by two bidentate nitrate anions and a coordinated EtOH molecule. It is interesting to note that all of the products formed between Zn(II), or Cd(II), and bptri exhibit a bis-pyridyl coordination environment despite the lack of steric hindrance at the 4-pyridyl donor. This is, presumably, a product of the angular nature of the bptri ligand that must infer favoured polymeric arrangements which involve the coordination of only two bptri ligands. A similar structural arrangement is observed for $[\text{Cd}(\text{b3ptz})(\text{NO}_3)_2(\text{MeOH})_2]_\infty$ [b3ptz = 1,4-bis(3-pyridyl)-2,3,5,6-tetrazine] [24]. A nitrate bridged $\text{Cd}(\text{NO}_3)_2$ -bptri species can also be prepared and this is discussed in Section 2.2.

Similarly to $[\text{Cd}(\text{NO}_3)_2(\text{bptri})(\text{EtOH})]_\infty$, 1,4-bis-(4-pyridyl)butadiyne (bpbdieyne) reacts with $\text{Co}(\text{NO}_3)_2$ to afford the 1D chain $[\text{Co}(\text{NO}_3)_2(\text{bpbdieyne})(\text{H}_2\text{O})_2]_\infty$ [25]. This species exists as 1D chains in which each Co(II) centre adopts a N_2O_4 coordination sphere with two monodentate nitrate, two water and two pyridyl donors (Fig. 3). The pyridyl donors come from two different bpbdieyne ligands which in turn bridge Co(II) centres generating the 1D chain

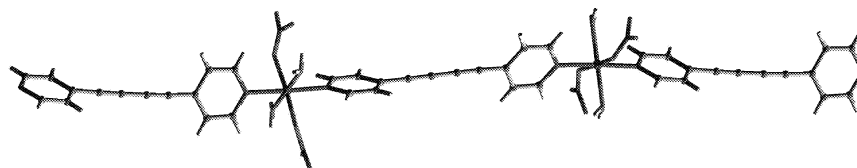


Fig. 3. View of the 1D chain formed by $[\text{Co}(\text{NO}_3)_2(\text{bpbdiyne})(\text{H}_2\text{O})_2]_\infty$ [25].

structure. This general motif, which involves bis-pyridyl, nitrate and solvent coordination at the metal centre, is relatively common and has also been observed for $[\text{Cd}(\text{NO}_3)_2(\text{bpbut})(\text{H}_2\text{O})_2]_\infty$, [bpbut = 1,4-bis(4-pyridyl)butane] [26], $[\text{Cd}(\text{NO}_3)_2(\text{b3pethyne})(\text{H}_2\text{O})_2]_\infty$, [b3pethyne = 1,2-bis(3-pyridyl)ethyne] [27] $[\text{Cu}(\text{NO}_3)_2(\text{bpethyne})(\text{MeOH})]_\infty$ [27], $[\text{Co}(\text{NO}_3)_2(\text{bptp})(\text{MeCN})]_\infty$, [bptp = bis(4-pyridyl)terephthalate] [21] and $[\text{Cu}(\text{NO}_3)_2(\text{bpanth})(\text{MeOH})]_\infty$ [bpanth] [22].

The ligand 1,2-bis(2-pyridyl)ethyne (b2pethyne) offers two pyridyl donors which are not sufficiently sterically inhibited to preclude metal coordination but the relative orientation of the ethyne inter-pyridyl bridge in relation to the N-donor group means that only two of these donors are accommodated around a single metal centre in combination with two coordinated nitrate anions [28]. In $[\text{M}(\text{NO}_3)_2(\text{b2pethyne})]_\infty$ ($\text{M} = \text{Co}, \text{Ni}, \text{Cu}$) the ligand acts as a transoid bridge to link metal centres into a 1D chain structure. However, using an alternative reaction solvent, EtOH vs. acetone, a dinuclear complex is formed, $\text{Cu}_2(\text{NO}_3)_4[\text{b2pethyne}]_3$, in which both one bridging and two monodentate b2pethyne ligands are observed [28]. This indicates that even a small degree of steric inhibition at the metal centre, in this case Cu(II), may lead to reduced bridging ability for a bidentate bipyridyl ligand.

A good example of the influence of steric inhibition is demonstrated by the product from the reaction of 2,4'-bipy with either $\text{Co}(\text{NO}_3)_2$ or $\text{Cd}(\text{NO}_3)_2$. The observed products, $[\text{Co}(2,4'\text{-bipy})_2(\text{NO}_3)_2(\text{H}_2\text{O})]_\infty$ and $[\text{Cd}(2,4'\text{-bipy})_2(\text{NO}_3)_2(\text{H}_2\text{O})_2]_\infty$, exhibit only 4-pyridyl coordination to the metal centre and thus only discrete molecular species are observed [29]. In both cases the 2-pyridyl group remains uncoordinated but is involved in intermolecular hydrogen-bonding interactions with coordinated H_2O molecules. This illustrates that the sterically hindered nature of the *ortho*-substituted pyridyl group allows competitive metal binding by H_2O and nitrate anions. However, under different conditions 2,4'-bipy can be forced to coordinate to Cd(II) through both the 4-pyridyl and 2-pyridyl groups affording a dinuclear metallacyclic species in which the seventh Cd(II) coordination site is occupied by a coordinated MeCN molecule [30].

The elongated analogue of 2,4'-bipy, 2,4'-(1,4-phenylene)bispyridine (2,4'-bpbh), reacts with both $\text{Zn}(\text{NO}_3)_2$ and $\text{Cd}(\text{NO}_3)_2$ to afford binuclear metallacycles, $[\text{M}(2,4'\text{-bpbh})(\text{NO}_3)_2]_2$, with both 2-pyridyl and 4-pyridyl groups coordinated to the metal centre (Fig. 4) [8]. In the case of the

Cd(II) compound, the higher coordination number exhibited by the metal centre, i.e. seven vs. six coordinate, results in the coordination of an additional ligand. In the presence of coordinating solvents, e.g. MeCN, DMF, ROH, the solvent provides the additional donor [30] but, in the absence of the other donors, a nitrate from one metallacycle bridges to an adjacent metallacycle resulting in the formation of a $[\text{Cd}(\text{NO}_3)]_\infty$ helix [8]. The case of nitrate bridging in this example will be discussed below in Section 2.2.

2.2. $\text{M}(\text{NO}_3)_2$ bis-pyridyl structures with nitrate bridging

Binuclear metallacycles, $[\text{M}(2,4'\text{-pyph})(\text{NO}_3)_2]_2$, are prepared from the reaction of 2,4'-bpbh with $\text{Cd}(\text{NO}_3)_2$ with both 2-pyridyl and 4-pyridyl groups coordinated to the metal centre (Fig. 4) [8]. In the absence of the other donors, the seven coordinate geometry exhibited by the Cd(II) centre results in nitrate bridging from one metallacycle to an adjacent metallacycle generating a $[\text{Cd}(\text{NO}_3)]_\infty$ helix. An extended structure is formed, constructed from $[\text{Cd}(2,4'\text{-bpbh})(\text{NO}_3)_2]_2$ metallacycles (Fig. 5). This framework is stable to guest removal and has the potential to act as a selective host material for separation processes.

Similar association of Cd-based metallacycles is also observed for the longer analogue of 2,4'-bpbh, 2,4'-(4-ethynylphenyl)bipyridyl (2,4'-bpacph). However, in this case

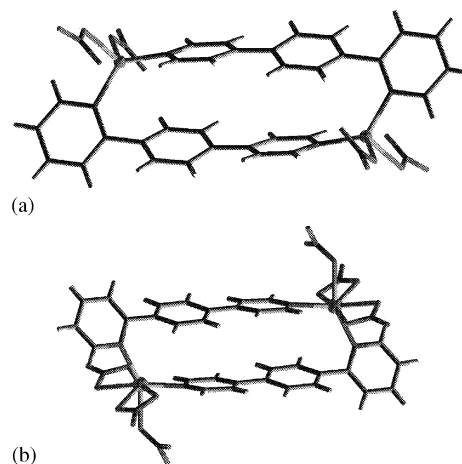


Fig. 4. View of metallacycles formed by (a) $[\text{Zn}(2,4'\text{-bpbh})(\text{NO}_3)_2]_2$ and (b) $[\text{Cd}(2,4'\text{-bpbh})(\text{NO}_3)_2]_2$ illustrating the additional binding of a bridging nitrate groups in the Cd(II) case [8].

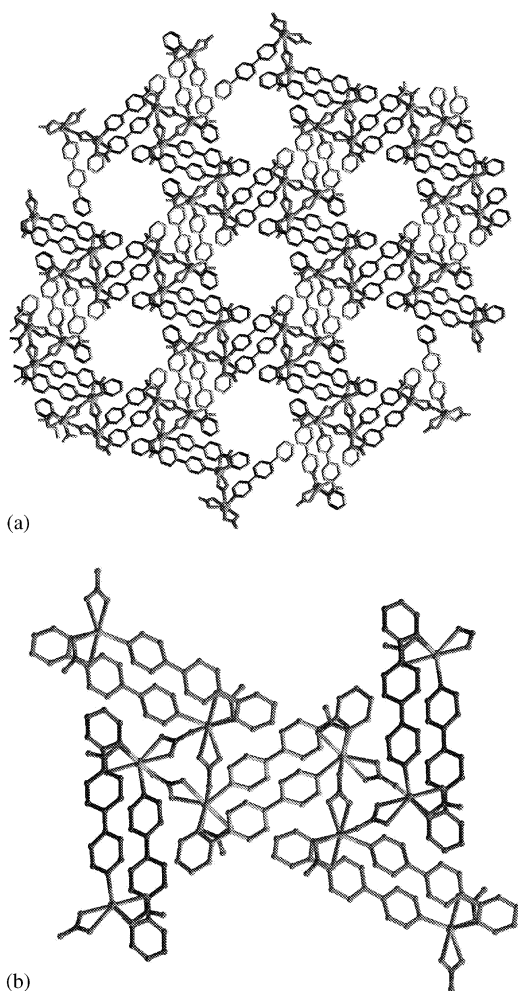


Fig. 5. View of (a) the 3D framework formed by $[\text{Cd}(2,4'\text{-biph})(\text{NO}_3)_2]_\infty$ generated through (b) nitrate bridging between adjacent metallacycles [8].

two different types of nitrate bridging are observed depending on the temperature of the reaction process [30]. At room temperature the $[\text{Cd}(\text{NO}_3)_2(2,4'\text{-bpacph})]_2$ metallacycles assemble in a homochiral fashion to give $\{[\text{Cd}(\text{NO}_3)_2(2,4'\text{-bpacph})]_2\}_\infty$ in which Cd(II) centres are linked by NO_3^- groups to form homochiral $[\text{Cd}(\text{NO}_3)]_\infty$ coordination chains which adopt a helical conformation. Two types of twofold helices are formed, P and M, each located around a crystallographic 2_1 screw axis (Fig. 6a). Each metallacycle interacts with four others and is engaged in both M and P helices. The nitrate-based inter-metallacyclic bridging affords a 2D sheet structure which contains equal numbers of P and M-helices.

This 2D coordination framework can be transformed, irreversibly, into a pseudo-polymorph via dispersal in a polar organic solvent mixture, *n*-BuOH/*o*-xylene, at elevated temperatures. The same binuclear metallacycles, $[\text{Cd}(\text{NO}_3)_2(2,4'\text{-bpacph})]_2$, are used in constructing a distinct coordination architecture but, in this case the nitrate groups bridge metallacycles in a *meso*-fashion (Fig. 6b). Consequentially each Cd(II) centre with a Δ arrangement

is linked through a bridging nitrate group to a Δ -Cd(II) centre such that linked Cd(II) centres are related by an inversion centre. As a result of this *meso*-nitrate bridging each metallacycle, $[\text{Cd}(\text{NO}_3)_2(2,4'\text{-bpacph})]_2$, interacts with only two others, compared to four for the low-temperature polymorph leading to a 1D chain of metallacycles [30]. Similar *meso*-association is observed for the highly related metallacycle $[\text{Cd}(\text{NO}_3)_2(2,4'\text{-bpphac})]_2$ [2,4'-bpphac = 2,4'-(2-ethynylphenyl)bipyridyl] when synthesised at elevated temperatures despite a slightly different nitrate bridging mode being adopted [30]. In contrast to $[\text{Cd}(\text{NO}_3)_2(2,4'\text{-bpacph})]_\infty$, the ligand 2,4'-pyphac can also form a mononuclear complex, $[\text{Cd}(\text{NO}_3)_2(2,4'\text{-bpphac})_2(\text{H}_2\text{O})]$, at room temperature. The Cd(II) centre is coordinated only by the less hindered 4-pyridyl donors while the 2-pyridyl donors remain uncoordinated. Nitrate bridging between Cd(II) cations arranges the $[\text{Cd}(\text{NO}_3)_2(2,4'\text{-pyphac})_2(\text{H}_2\text{O})]$ units into a 1D polymer. Significantly, this 1D chain $[\text{Cd}(\text{NO}_3)_2(2,4'\text{-bpphac})_2(\text{H}_2\text{O})]_\infty$ can be converted irreversibly to $[\text{Cd}(\text{NO}_3)_2(2,4'\text{-bpphac})]_\infty$ at 120 °C.

A similar nitrate bridging mode to that observed in $[\text{Cd}(\text{NO}_3)_2(2,4'\text{-bpphac})_2(\text{H}_2\text{O})]_\infty$ is also observed in $[\text{Cd}(\text{NO}_3)_2(\text{bpbdine})(\text{H}_2\text{O})]_\infty$ but, in this case both ends of the bipyridyl donor (both 4-pyridyl donors) are bound to Cd(II) centres such that a 2D coordination framework is constructed (Fig. 7) [25]. This motif is also observed in one form of $[\text{Cu}(\text{NO}_3)_2(\text{bpethyne})]_\infty$ [bpethyne = 1,2-bis(4-pyridyl)ethyne] [31] but a further product is formed from the reaction of $\text{Cu}(\text{NO}_3)_2$ with bpethyne which adopts a tetrakis-pyridyl coordination geometry which will be discussed in Section 4.

Nitrate bridging is particularly common amongst $\text{Cd}(\text{NO}_3)_2$ species and this leads to a particularly unusual compound from the reaction of this salt with bptri [23]. Reaction between $\text{Cd}(\text{NO}_3)_2$ and bptri forms a range of products depending on reaction solvent and M:L reaction ratio and some of these are discussed in Section 2.1. Reaction of a 1:1 ratio of $\text{Cd}(\text{NO}_3)_2$ with bptri in MeCN/ CH_2Cl_2 affords the complex $[\text{Cd}_2(\text{NO}_3)_4(\text{bptri})_2(\text{MeCN})]_\infty$ which exists as a doubly interpenetrated 4.8^2 2D sheet in the solid-state (Fig. 8). Four distinct Cd(II) ions are observed in the crystallographic asymmetric unit and are each coordinated by two bptri ligands which link adjacent Cd(II) centres. Two pairs of Cd(II) centres are formed; a formally monocationic ' $\text{Cd}_2(\text{NO}_3)_3(\text{MeCN})_2$ ' unit and a formally mononegative ' $\text{Cd}_2(\text{NO}_3)_5$ ' unit (Scheme 3). The bptri bridging generates $[\text{Cd}(\text{bptri})]_4$ metallacycles which are bridged via nitrate anions into a 2D sheet with topology 4.8^2 . Thus, the $[\text{Cd}(\text{bptri})]_4$ metallacycles form a cyclic unit with four nodes and the nitrate bridges lead to further cyclic units with eight nodes around which bptri and nitrate bridges alternate. The large spaces generated within each metallacycle (ca. 20×17 Å) allows parallel interpenetration of two of these 2D sheets.

Other examples of bis-pyridyl donor coordination spheres have been observed but these are within multi-component architectures and, therefore, will be discussed in Section 5.

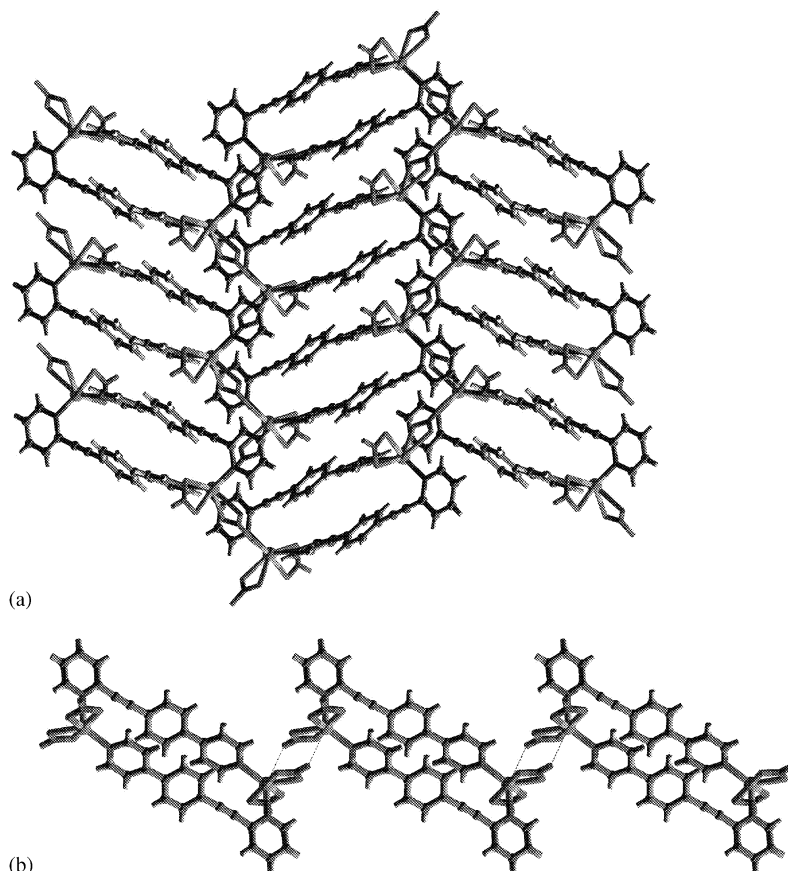


Fig. 6. View of the extended structures formed via nitrate bridging in (a) $\{[\text{Cd}(\text{NO}_3)_2(2,4'\text{-bpacph})]_2\}_\infty$ in which homochiral $[\text{Cd}(\text{NO}_3)]_\infty$ coordination chains are observed leading to a 2D sheet and (b) $[\text{Cd}(\text{NO}_3)_2(2,4'\text{-bpacph})]_2$ in which *meso*-nitrate bridging generates a 1D chain [30].

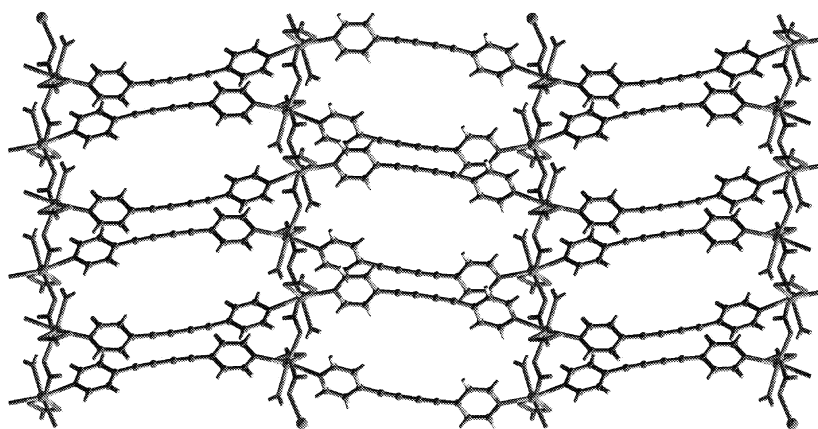


Fig. 7. View of the 2D sheet structure formed by $[\text{Cd}(\text{NO}_3)_2(\text{bpbdiyne})(\text{H}_2\text{O})]_\infty$ generated by nitrate bridging [25].

3. $\text{M}(\text{NO}_3)_2$ tris-pyridyl structures—T-shaped connecting nodes

$\text{M}(\text{NO}_3)_2$ units were first recognised as a feasible source of T-shaped connectivity by Fujita et al. [32] building on the first structural characterisation of $\text{Co}(\text{py})_3(\text{NO}_3)_2$, $\text{Zn}(\text{py})_3\text{f}(\text{NO}_3)_2$ and $\text{Cd}(\text{py})_3(\text{NO}_3)_2$, (py = pyri-

dine) [33]. It is clear from the single crystal X-ray structures of these mononuclear complexes that the pyridine donors are arranged in a near perfect T-shape. Therefore, it was hypothesised that replacement of these pyridine donors with bridging bipyridyl ligands should afford extended structures based upon the T-shaped building-block.

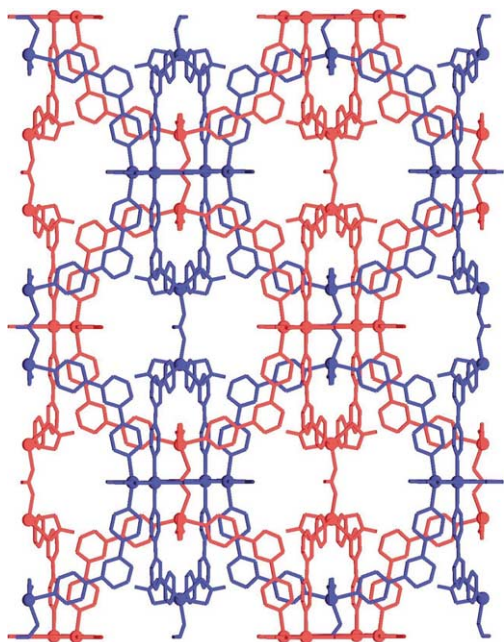


Fig. 8. View of the doubly interpenetrated 4.8^2 2D sheets formed by $[\text{Cd}_2(\text{NO}_3)_4(\text{bptri})_2(\text{MeCN})]_\infty$ [23].

3.1. Potential architectures using T-shaped connecting nodes

The T-shaped connecting node is particularly flexible in terms of the connectivities that can be adopted by the extended polymeric structures that it forms. These range from 1D to 2D and 3D arrays (Scheme 4). Perhaps the simplest system is the molecular ladder structure (Scheme 4a) in which those ligands that are *trans* to each other at each T-shaped metal junction are linked into a $(\text{ML})_\infty$ chain, forming the struts of the ladder, with the orthogonal ligand, acting as rungs, linking these chains into the ladder arrangement.

The brickwall structure (Scheme 4b) is highly related to the ladder motif except that the 'rung' ligands are positioned on opposing sides of the $(\text{ML})_\infty$ chains formed by the *trans* bipyridyl ligands. This then forms a 2D sheet structure.

The bilayer structure (Scheme 4c) is highly related to both the ladder and the brickwall arrangement. In this instance $(\text{ML})_\infty$ chains are again formed using the *trans* bipyridyl ligands and, in this case, the orthogonal ligand links these chains such that all of the orthogonal ligands are positioned

on adjacent sides of a given $(\text{ML})_\infty$ chain. However, in contrast to the ladder structure the $(\text{ML})_\infty$ chains on opposing ends of an orthogonal rung ligand propagate in perpendicular directions leading to the formation of the 2D array.

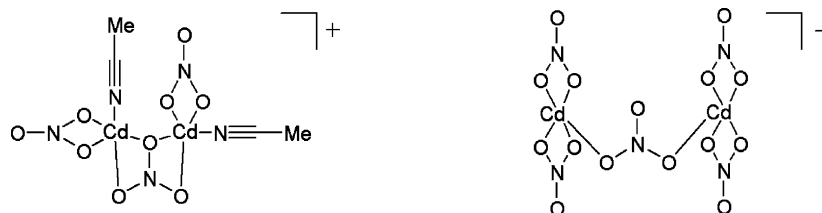
The herringbone motif (Scheme 4d) is most highly related to the brickwall structure in that the architecture adopted is a 2D sheet structure with (6,3) topology. However, in this instance no $(\text{ML})_\infty$ chains are formed but the maximum length of any near-linear metal-bipyridyl chain contains four metals and three ligands, i.e. (M_4L_3) . The two terminal metal nodes of these (M_4L_3) chains act as caps to this short chain by using the orthogonally arranged ligand of the $\text{M}(\text{NO}_3)_2\text{L}_3$ node. The two central metals of the (M_4L_3) chain use the two mutually *trans* ligands at the metal node but their orthogonal ligands face opposing sides of the (M_4L_3) chain and as such the herringbone motif is generated.

Two 3D architectures have been observed, thus far, using T-shaped connecting nodes (Scheme 4e and f). Although only two examples of 3D architectures have been observed [34,49] using T-shaped nodes these are just the first members of many possible 3D arrangements.

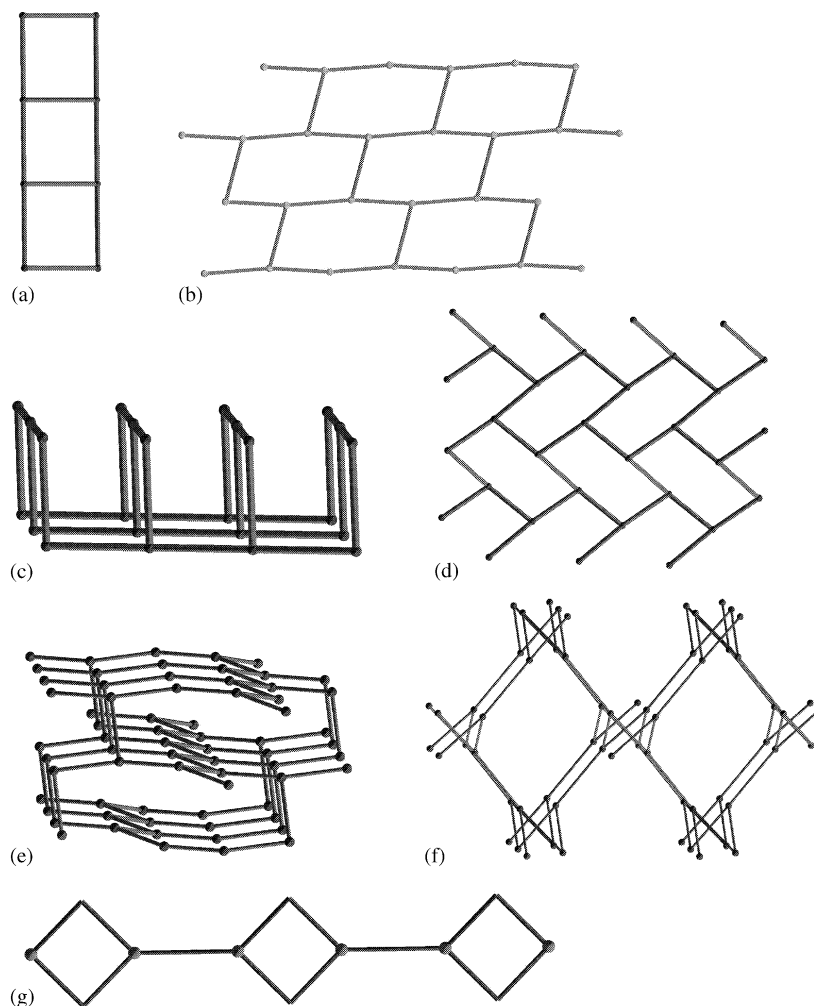
If an angular ligand is used it is also possible to generate a 1D chain structure with T-shaped tris-pyridyl nodes, Scheme 4g. The chain consists of alternating double bridges and single bridges and the angular ligand is required to generate the $(\text{ML})_2$ metallacyclic sub-units.

3.2. Coordination frameworks observed with T-shaped connecting nodes

The range of architectures built from T-shaped connecting nodes outlined in Section 3.1 are observed for a range of $\text{M}(\text{NO}_3)_2$ salts. The flexibility of this type of node is reflected in the fact that for all of the metal salts studied thus far [$\text{M} = \text{Co}(\text{II})$, $\text{Ni}(\text{II})$, $\text{Zn}(\text{II})$, or $\text{Cd}(\text{II})$] at least two of these structural types have been observed and in some instances, most noticeably $\text{Co}(\text{II})$, all of them have been observed. In some cases at least three of the architectures shown in Scheme 4 have been observed for a single $\text{M}(\text{NO}_3)_2$ salt and a given ligand. This illustrates the subtle energy balance that clearly exists between these different motifs and the complexity of studying these systems. The following section is sub-divided on the basis of the particular $\text{M}(\text{NO}_3)_2$ salt used so that the complexity of a given metal/ligand combination can be readily seen. However, the motifs that have been observed are also discussed in Section 3.3 to give an overview



Scheme 3. Formally monocationic ' $\text{Cd}_2(\text{NO}_3)_3(\text{MeCN})_2$ ' and mononegative ' $\text{Cd}_2(\text{NO}_3)_5$ ' units observed in the 4.8^2 2D sheet formed by $[\text{Cd}_2(\text{NO}_3)_4(\text{bptri})_2(\text{MeCN})]_\infty$ [23].



Scheme 4. Structural motifs observed with T-shaped connecting $M(\text{NO}_3)_2$ nodes. (a) ladder; (b) brickwall; (c) bilayer; (d) herringbone; (e) 3D [34]; (f) 3D [49]; (g) double/single chain.

of the different $M(\text{NO}_3)_2$ salts and ligands that can be used to generate a given T-shaped architecture.

3.2.1. Cobalt (II) nitrate architectures

$\text{Co}(\text{NO}_3)_2$ reacts with 4,4'-bipyridine (4,4'-bipy) in either $\text{MeOH}/\text{CHCl}_3$, or MeOH/MeCN , to afford the complex $[\text{Co}_2(\text{NO}_3)_4(4,4'\text{-bipy})_3]_\infty$ which exhibits a molecular ladder motif (Fig. 9) [36].

It can be seen that the role of the nitrate anion in this $\text{Co}(\text{II})$ system is crucial in determining the overall topology

of the molecular ladder. By coordinating both nitrates in a pseudo-bidentate fashion, either by a symmetrical bidentate or using an unsymmetrical coordination mode in which one $\text{Co}-\text{O}$ bond is elongated, the $\text{Co}(\text{II})$ centre fills four of its seven coordination sites of a pentagonal bipyramid leaving three available sites for N-donor coordination which are orientated in a T-shaped arrangement. Thus, the nitrate anions are crucial in determining the basic connectivity of the extended structure.

Despite the cavity between the rungs of the $[\text{Co}_2(\text{NO}_3)_4(4,4'\text{-bipy})_3]_\infty$ ladder being large enough to allow interpenetration of further ladders, the structure exhibits no such interpenetration but rather includes guest solvent molecules. When grown from a $\text{MeOH}/\text{CHCl}_3$ solvent mixture, the CHCl_3 molecules are included in the structure and participate in weak H-bonding interactions with both the NO_3^- anions and the 4,4'-bipy ligands which gives some indication of the reason for the lack of interpenetration. However, when crystallised from a MeOH/MeCN mixture the MeCN molecules are clathrated within the ladder

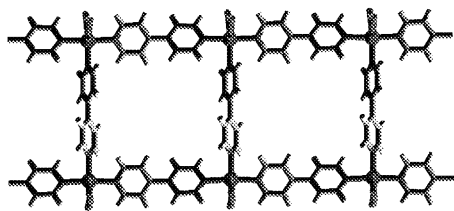


Fig. 9. View of the ladder structure formed by $[\text{Co}_2(\text{NO}_3)_4(4,4'\text{-bipy})_3]_\infty$ illustrating a T-shaped tris-pyridyl coordination mode [36].

structure instead of the potentially H-bonding MeOH molecules. This indicates that guest inclusion can be driven by shape/size selectivity rather than by other weaker forces and illustrates the subtle energy balance that presumably controls the network structure. It is worth noting that $\text{Co}(\text{NO}_3)_2$ reacts with 1,2-bis(4-pyridyl)ethane (bpeth) to afford a non-interpenetrated molecular ladder when crystallised from MeOH/ CHCl_3 (see below) [37].

A similarly non-interpenetrated ladder is also observed for the much longer ligand 2,5-bis(4-pyridyl)-3,4-diaza-2,4-hexadiene (bpdahd) when prepared from a $\text{CH}_2\text{Cl}_2/\text{MeOH}$ layered solvent mixture. In contrast, replacing the CH_2Cl_2 with benzene in this reaction affords a tetrakis-pyridyl based square-grid structure which will be discussed in Section 4.2 [38].

Solvent templating has been observed in $\text{Co}(\text{NO}_3)_2$ -bipyridyl systems illustrating that although the nitrate anion can essentially control the local connectivity of the network the extended structure is dependent on more subtle effects.

Reaction of $\text{Co}(\text{NO}_3)_2$ with 4,4'-bipyridyl in the presence of templating agents affords different structural motifs. By incorporating either CS_2 [39] or H_2O [12] into the crystallisation reaction affords a molecular bilayer motif, $[\text{Co}_2(\text{NO}_3)_4(4,4'\text{-bipy})_3]_\infty$ (Fig. 10), in which each Co(II) centre still acts as a T-shaped connecting junction with the nitrate anions acting to block four of the seven available coordination sites. The desolvated network has been shown to be stable to guest removal and allows adsorption of CH_4 , N_2 and O_2 with a particular affinity for CH_4 reflecting the organic periphery of the host channels [12].

From the reaction of $\text{Co}(\text{NO}_3)_2$ with 4,4'-bipyridyl in the presence of a pyridine template a further structural motif is observed (Fig. 11) [34]. In this case a 3D lattice is observed (Scheme 4e) even though the same local geometry is found at the metal centre. In this structure, the T-shaped connections are arranged such that pairs are oriented at 180° with respect to each other and then at 90° to the adjacent pair of connections. The 3D lattice is triply interpenetrated but leaves channels that are occupied by guest solvent molecules.

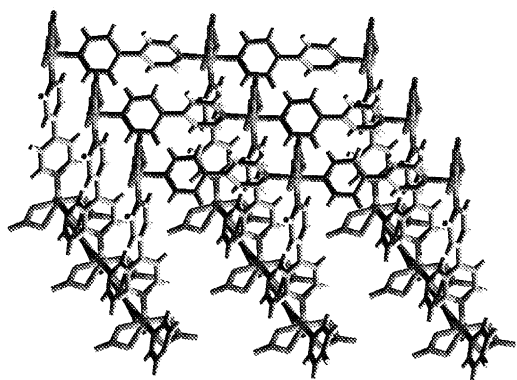


Fig. 10. View of the bilayer structure formed by $[\text{Co}_2(\text{NO}_3)_4(4,4'\text{-bipy})_3]_\infty$ illustrating an alternative architecture generated using the T-shaped tris-pyridyl coordination mode [12,39].

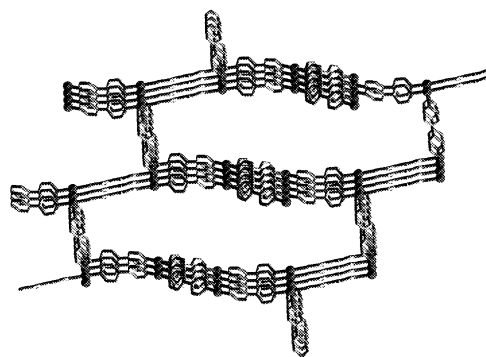


Fig. 11. View of the 3D architecture generated by $[\text{Co}_2(\text{NO}_3)_4(4,4'\text{-bipy})_3]_\infty$ from the reaction of $\text{Co}(\text{NO}_3)_2$ with 4,4'-bipyridyl in the presence of a pyridine template [34].

A 3D structure is also generated from, ostensibly, T-shaped nodes in $[\text{Co}_2(\text{NO}_3)_4(\text{b3pdabd})_3]_\infty$ [b3pdabd = 1, 4-bis(3-pyridyl)-2,3-diaza-1,3-butadiene] (Scheme 4f) [49]. In this case, however, despite a T-shaped arrangement of pyridyl donors at the Co(II) centre, the orientation of the angular ligands gives rise to a severely distorted arrangement of the pyridyl donors at the opposing ends of the ligands coordinated to any given metal node (Fig. 12). This gives rise to a highly unusual 3D framework in which Co-ligand 'columns' (Fig. 12b) are arranged, along the crystallographic *c*-axis, using two of the bridging bipyridyl ligands and these are then bridged in the *ab*-plane by the remaining bipyridyl ligand. This unusual structure exhibits fourfold interpenetration filling the large void space within any given framework.

Upon reaction with $\text{Co}(\text{NO}_3)_2$ the ligand bpeth, in a 1:3 ratio, affords three different coordination networks depending upon the templating conditions used [37]. When crystallised from MeOH/MeCN the complex, $[\text{Co}_2(\text{NO}_3)_4(\text{bpeth})_3]_\infty$, illustrated in Fig. 13a is isolated. The nitrate anions are coordinated forming a T-shaped junction but, in this case, the bpeth ligand is flexible and can adopt either *gauche* or *anti* isomers. In this complex two ligands adopt a *gauche* arrangement linking two $\text{Co}(\text{NO}_3)_2$ units forming a box-shaped unit which are then linked by ligands in the *anti* arrangement into a 1D polymer, Scheme 4g. In complete contrast, if the crystallisation process is performed in MeOH/MeCN but in the presence of a ferrocene templating agent, a molecular bilayer structure (Scheme 4c) is formed (Fig. 13b). For every ligand in a *gauche* conformation two ligands in an *anti* conformation are observed in the structure. The ligands in the *anti* arrangement bridge T-shaped $\text{Co}(\text{NO}_3)_2$ junctions in a linear arrangement and these chains are then linked through the *gauche* ligand to form the bilayer structure. By varying the solvent combination to MeOH/ CHCl_3 the more familiar molecular ladder motif (Scheme 4a) is formed in which the ligands all adopt *anti* conformations. As with the 4,4'-bipy analogue of this complex [36] the spaces between the rungs of the ladder are filled with guest CHCl_3 solvent molecules which inhibit interpenetration of adjacent ladders.

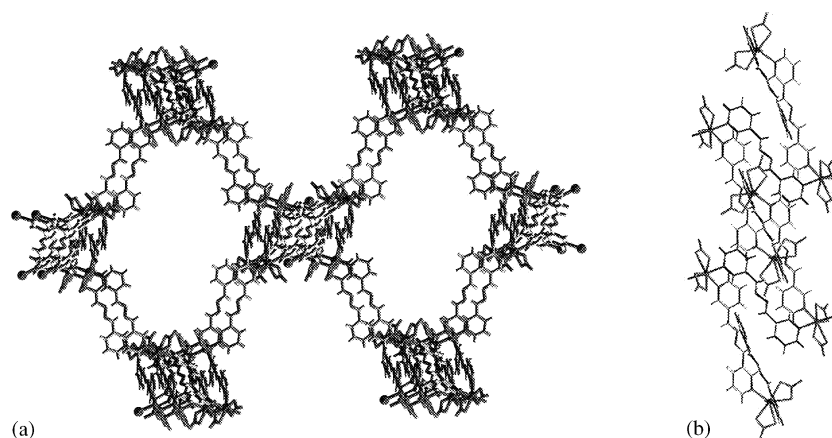


Fig. 12. View of (a) the 3D structure generated by $[\text{Co}_2(\text{NO}_3)_4(\text{b3pdabd})_3]_\infty$ in which the angular nature of the ligand gives rise to a severely distorted arrangement T-shaped connecting arrangement at any given metal node; (b) view of the Co-ligand 'columns' arranged, along the crystallographic c -axis, which are bridged in the ab -plane by the remaining bipyridyl ligand to give the 3D structure shown in (a) [49].

Trans-1,2-bis(4-pyridyl)-ethylene (bpethene) also reacts with $\text{Co}(\text{NO}_3)_2$ to afford a ladder architecture, $[\text{Co}_2(\text{NO}_3)_4(\text{bpethene})_3]_\infty$ which can be converted to a mononuclear species, $[\text{Co}(\text{H}_2\text{O})_4(\text{bpe})_2](\text{NO}_3)_2$, under moist conditions [40]. The mononuclear complex which adopts an octahedral Co(II) coordination sphere with four water ligands and two monodentate bpe ligands can be converted to the ladder complex by heating the solid above 150°C .

The linear, unsaturated analogue of bpeth, bpethyne has also been studied in combination with $\text{Co}(\text{NO}_3)_2$ and illustrates the extremely subtle balance between the different structural isomers of complexes formed between $\text{Co}(\text{NO}_3)_2$ units and bipyridyl ligands with the formula $[\text{Co}_2(\text{NO}_3)_4(\text{bpethyne})_3]_\infty$ [41,42]. Again, two reaction

products have been structurally characterised, the familiar molecular ladder motif (Scheme 4a) and a new herringbone structure (Scheme 4d) which is another structural motif exhibited by the T-shaped junction. Single crystals of the two isomeric products can be grown from the same reaction mixture (MeOH/MeCN) [41] but samples of pure molecular ladder can be isolated from an acetone–ethanol mixture (Fig. 14) [42]. The molecular ladder structure is analogous to that observed in the previous examples with the nitrate anions again generating a T-shaped geometry at the metal centre except that the ladders interpenetrate in a perpendicular fashion to afford a polycatenated 3D structure. Each square-space between the rungs of the ladder is filled by two other square units from two further perpendicular ladders.

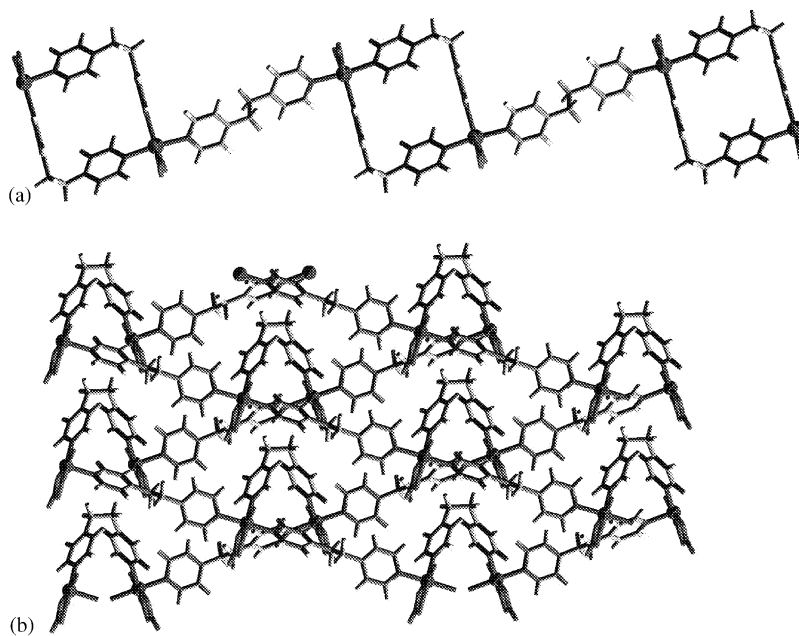


Fig. 13. Views of (a) the double/single bridged 1D chain formed by $[\text{Co}_2(\text{NO}_3)_4(\text{bpeth})_3]_\infty$ and (b) a bilayer structure formed by $[\text{Co}_2(\text{NO}_3)_4(\text{bpeth})_3]_\infty$ but using alternative reaction conditions [37].

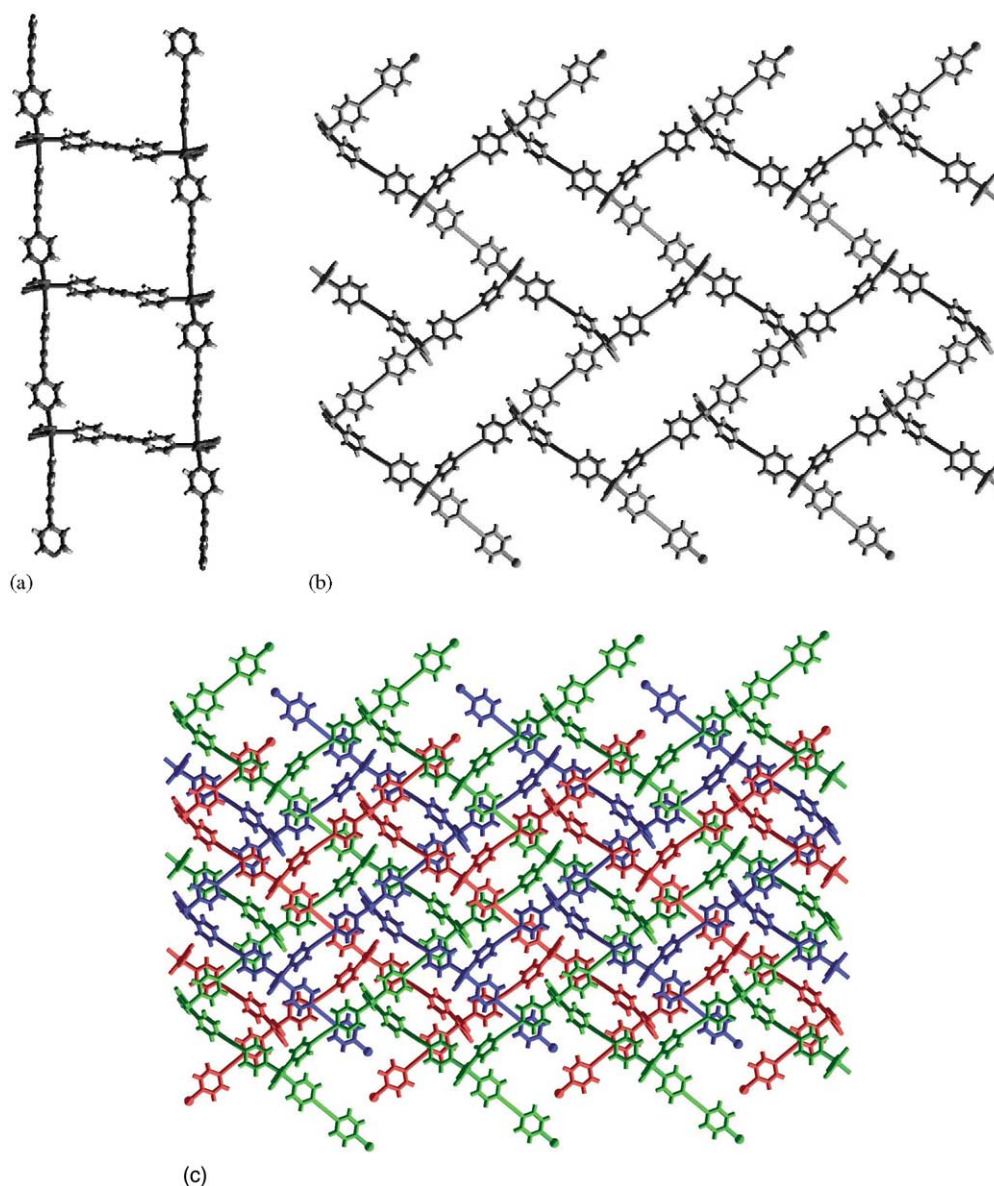


Fig. 14. Views of structures formed by $[\text{Co}_2(\text{NO}_3)_4(\text{bpethyne})_3]_\infty$ (a) ladder (b) herringbone and (c) triple parallel interpenetration observed in the herringbone complex [41,42].

The herringbone structure similarly adopts a T-shaped arrangement at the Co(II) centre but, in this case, the orientation of the ligands affords an entirely different structural motif. Each of these herringbone sheets undulates allowing triple parallel interpenetration giving rise to a polycatenated 2D sheet (Fig. 14c) [41]. Powder X-ray diffraction studies of the products from simple precipitation reactions of bpethyne and $\text{Co}(\text{NO}_3)_2$ yield intriguing results [42]. If an acetone solution of $\text{Co}(\text{NO}_3)_2$ is added to a solution of the ligand in EtOH then pure samples of the interpenetrating molecular ladder compound can be prepared but, if the addition process is reversed, then powder X-ray studies reveal that the product is ca. 20% molecular ladder and 80% of a further structural motif, the brickwall, (Scheme 4b). These results

further reinforce the subtle differences between the different structural types based on the $\text{Co}(\text{NO}_3)_2$ unit.

The herringbone motif is also observed when $\text{Co}(\text{NO}_3)_2$ is reacted with *trans*-4,4'-azobis(pyridine) (azpy) to afford $[\text{Co}_2(\text{NO}_3)_4(\text{azpy})_3]_\infty$ [43]. As with $[\text{Co}_2(\text{NO}_3)_4(\text{bpethyne})_3]_\infty$ [41] the T-shaped arrangement at the Co(II) centre leads to undulating herringbone sheets which are triply interpenetrated in a parallel fashion [43]. The corresponding brickwall structure has also been reported for this compound [44] when using a EtOH/ Me_2CO reaction mixture instead of EtOH/ CH_2Cl_2 for the herringbone structure. In contrast to the triple interpenetration observed for the herringbone structure the brickwall structure adopts quadruple interpenetration in a parallel fashion [44].

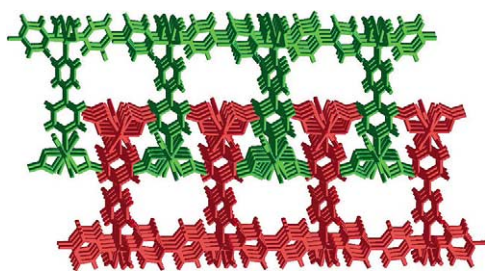


Fig. 15. View of the interdigitation between bilayer architectures in $[\text{Ni}_2(\text{NO}_3)_4(4,4'\text{-bipy})_3]_\infty$ [9,12].

In contrast to these interpenetrated herringbone structures, the significantly longer ligands 1,2-bis(4-pyridyl)-2,3-diaza-1,3-butadiene (bpdabd) [38] and b3pdabd [35] react with $\text{Co}(\text{NO}_3)_2$ to afford brickwall structures, $[\text{Co}_2(\text{NO}_3)_4(\text{L})_3]_\infty$, which do not exhibit interpenetration despite large cavities within the brickwall sheet.

3.2.2. Nickel (II) nitrate architectures

$\text{Ni}(\text{NO}_3)_2$ also acts as a T-shaped connecting unit in the same manner as $\text{Co}(\text{NO}_3)_2$ and again this reflects the arrangement observed in $[\text{Ni}(\text{NO}_3)_2(\text{py})_3]$ [33]. Reaction of $\text{Ni}(\text{NO}_3)_2$ with 4,4'-bipy in a 2:3 ratio affords a complex, $[\text{Ni}_2(\text{NO}_3)_4(4,4'\text{-bipy})_3]_\infty$, which has been structurally characterised by both powder [12] and single crystal [9] X-ray diffraction. Both techniques confirm a molecular bilayer structure, Scheme 4c. The bilayer structure forms large 'grooves' which accommodate interdigitated castellations from adjacent bilayers (Fig. 15). This complex exhibits interesting properties in that it is stable to the loss of guest solvent molecules as evidenced by single crystal X-ray studies of the desolvated network [9]. This desolvated material has been shown to adsorb CH_4 , O_2 , N_2 [12], CO_2 and N_2O gases [10], water and alcoholic solvents [9,10].

Reaction of $\text{Ni}(\text{NO}_3)_2$ with *trans*-4,4'-azobis(pyridine) in a 1:2 ratio affords a complex network structure which exhibits two interpenetrating networks; one with tris-pyridyl nodes and one with tetrakis-pyridyl nodes [45]. This structure will be discussed in more detail in Section 5.

3.2.3. Zinc(II) nitrate architectures

T-shaped $\text{Zn}(\text{NO}_3)_2$ junctions are observed in the single crystal X-ray structure of the product of the reaction with bpethyne, $[\text{Zn}_2(\text{NO}_3)_4(\text{bpethyne})_3]_\infty$ [42]. This complex adopts the interpenetrating molecular ladder structure in the same manner as its Co(II) analogue. However, powder X-ray diffraction analysis of the bulk product indicated that the product was actually a mixture of both ladders, Scheme 4a, and a more dominant component of the brick-wall type structure, Scheme 4b [42].

Non-interpenetrated molecular ladders, $[\text{Zn}_2(\text{NO}_3)_4(\text{L})_3]_\infty$, are formed from the reaction of $\text{Zn}(\text{NO}_3)_2$ with either 4,4'-bipy [46] or b3ptz [24]. $\{[\text{Zn}_2(\text{NO}_3)_4(4,4'\text{-bipy})_3] \cdot 0.5\text{pyrene} \cdot \text{MeOH}\}_\infty$ is prepared from the reaction of $\text{Zn}(\text{NO}_3)_2$ with 4,4'-bipy and pyrene in MeOH [46]. A

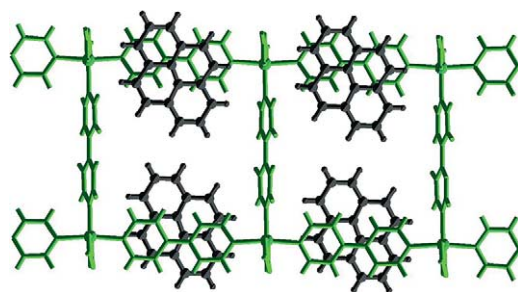


Fig. 16. View of the accommodation of pyrene in the ladder polymer $[\text{Zn}_2(\text{NO}_3)_4(4,4'\text{-bipy})_3]_\infty$ [46].

ladder motif is adopted by the $[\text{Zn}_2(\text{NO}_3)_4(4,4'\text{-bipy})_3]_\infty$ coordination polymer and the pyrene molecules are sandwiched between 4,4'-bipy molecules on adjacent ladders (Fig. 16). The isolation of the pyrene molecule in this specific environment results in strong fluorescence which has been assigned as a 2:1 4,4'-bipy:pyrene exciplex fluorescence. As with $[\text{Co}_2(\text{NO}_3)_4(4,4'\text{-bipy})_3]_\infty$ and $[\text{Ni}_2(\text{NO}_3)_4(4,4'\text{-bipy})_3]_\infty$, $[\text{Zn}_2(\text{NO}_3)_4(4,4'\text{-bipy})_3]_\infty$ has also been prepared in the bilayer structure form, Scheme 4c, from an EtOH/acetone solvent mixture and the desolvated structure has been shown to absorb CH_4 , N_2 and O_2 gases [12].

Solvent dependence is also observed for the reactions of $\text{Zn}(\text{NO}_3)_2$ with b3ptz. When b3ptz is reacted with $\text{Zn}(\text{NO}_3)_2$ in an EtOH (or $i\text{PrOH}$) CH_2Cl_2 mixture each Zn(II) centre adopts the expected T-shaped motif which is utilised in the formation of the ladder coordination polymer $[\text{Zn}_2(\text{NO}_3)_4(\text{b3ptz})_3]_\infty$ [24]. However, the T-shaped geometry at the Zn(II) centre is disrupted when MeOH is used as the alcoholic solvent. The MeOH molecule coordinates to the metal centre allowing only two residual sites for pyridyl coordination. This results in the formation of a hydrogen-bonded 1D polymer which falls outside the remit of this article [24].

3.2.4. Cadmium (II) nitrate architectures

In contrast to the large range of tris-pyridyl architectures characterised for $[\text{Co}_2(\text{NO}_3)_4(4,4'\text{-bipy})_3]_\infty$, only one analogous structure has been reported for $[\text{Cd}_2(\text{NO}_3)_4(4,34'\text{-bipy})_3]_\infty$ a bilayer structure [47] topologically identical to those observed for $[\text{M}_2(\text{NO}_3)_4(4,4'\text{-bipy})_3]_\infty$ ($\text{M} = \text{Co}, \text{Ni}, \text{Zn}$) [9,10,12]. $\text{Cd}(\text{NO}_3)_2$ tetrakis-4,4'-bipy complexes are more common but will be discussed in Section 4.

Molecular ladders were described for the first time by Fujita and were prepared from the reaction of $\text{Cd}(\text{NO}_3)_2$ and 1,4-bis(4-pyridyl)methyl-benzene (bpmb) in a 2:3 ratio [32]. The complex $[\text{Cd}_2(\text{NO}_3)_2(\text{bpmb})_3]_\infty$ exhibits the molecular ladder motif with each Cd(II) centre sitting in a heptacoordinate environment. The lengthy nature of the bpmb ligand results in the formation of large, 60-membered rings generating large cavities between the rungs of the ladder. These cavities allow interpenetration of adjacent ladders in a perpendicular fashion generating an interlocked 3D

structure. Each ring within a ladder is catenated by four other rings from independent ladders. Reaction in the presence of 1,4-dibromobenzene results in the clathration of the guest aromatic compound without loss of interpenetration [48].

However, as with the Co(II) systems, it can be seen from the highly related complex $[\text{Cd}_2(\text{NO}_3)_2(\text{bpmfb})_3]_\infty$ [$\text{bpmfb} = 1,4\text{-bis}(4\text{-pyridyl})\text{methyl-}2,3,5,6\text{-tetrafluorobenzene}$] [32] that although the nitrate can affect the local cadmium environment the overall network topology is controlled by more subtle effects. The Cd(II) centre still sits in a local heptacoordinate environment with the three coordinated pyridyl donors in a T-shaped arrangement. However, in this case the extended polymer forms a brickwall motif, Scheme 4b. These brickwall sheets are triply interpenetrated in a parallel fashion to give an overall interwoven 2D sheet. This is the same mode of interpenetration observed for the herringbone sheets in both $[\text{Co}_2(\text{NO}_3)_4(\text{bpethyne})_3]_\infty$ [41] and $[\text{Co}_2(\text{NO}_3)_4(\text{azpy})_3]_\infty$ [43].

Brickwall structures are also observed for $[\text{Cd}_2(\text{NO}_3)_4(\text{b3pdabd})_3]_\infty$ [35,49], $\{\text{Cd}_2(\text{NO}_3)_4(\text{bpsfb})_3\}_\infty$ [$\text{bpsfb} = 2,3,5,6\text{-tetrafluoro-}1,4\text{-bis}(4\text{-pyridyl-sulfonyl})\text{benzene}$] [50] and $[\text{Cd}_2(\text{NO}_3)_4(\text{bpob})_3]_\infty$ [$\text{bpob} = 1,4\text{-bis}(4\text{-pyridoxy})\text{benzene}$] [51]. In the case of $[\text{Cd}_2(\text{NO}_3)_4(\text{b3pdabd})_3]_\infty$, the angles adopted by the 3-pyridyl substituted ligand results in a significant distortion leading to a highly distorted structure which the authors describe as a ‘polycyclohexane network’ (Fig. 17) [35]. Despite the distortion of the $[\text{Cd}_2(\text{NO}_3)_4(\text{b3pdabd})_3]_\infty$ sheet, no interpenetration is observed and the framework can reversibly desorb guest molecules without framework decomposition. This structure is analogous to that observed for the corresponding Co(II) complex [35].

As with $[\text{Cd}_2(\text{NO}_3)_4(\text{b3pdabd})_3]_\infty$, the product from the reaction of 1,3-bis(4-pyridyl)propane (bppro) with

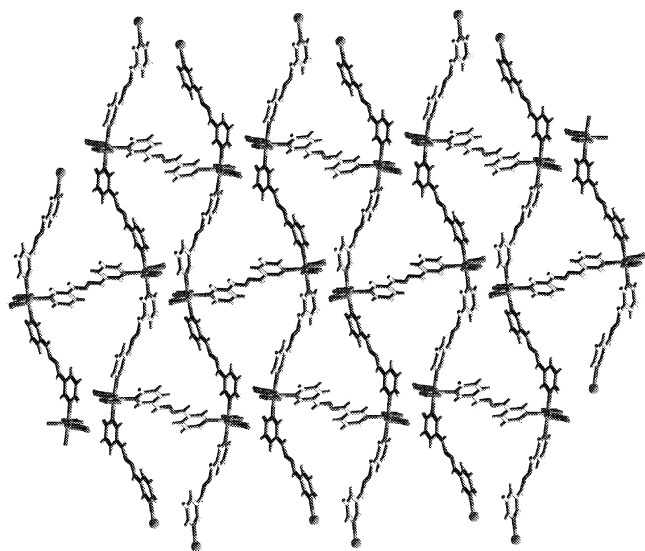


Fig. 17. View of the ‘polycyclohexane network’ formed by $[\text{Cd}_2(\text{NO}_3)_4(\text{b3pdabd})_3]_\infty$ which is significantly distorted from a more conventional brickwall arrangement by the angles adopted by the 3-pyridyl substituted ligand [35].

$\text{Cd}(\text{NO}_3)_2$ affords a 2D sheet of (6,3) topology, $[\text{Cd}_2(\text{NO}_3)_4(\text{bppro})_3]_\infty$, which exhibits fourfold interpenetration. The flexibility of the ligand leads to some ambiguity with the nomenclature ascribed to this framework but the network is closer to the herringbone motif than the brickwall structure [52].

Combination of the $\text{Cd}(\text{NO}_3)_2$ junction with the flexible ligand bpeth affords a 1D polymer in which the compound adopts an alternating single-bridged/double-bridged motif, Scheme 4g [53]. A box-shaped unit is formed by linking two $\text{Cd}(\text{NO}_3)_2$ junctions through two ligands in a *gauche* conformation which are subsequently linked by ligands in the *anti* arrangement to generate the 1D polymer.

The reactions between $\text{Cd}(\text{NO}_3)_2$ and the longer linear bipyridyl ligands, bpethyne [42,54], azpy [43], b3ptz [24] and 1,4-bis(4-pyridyl)-2,3,5,6-tetrazine (bptz) [55] have also been investigated.

Combination of $\text{Cd}(\text{NO}_3)_2$ and bpethyne building-blocks [42,54] affords either perpendicularly-interpenetrating molecular ladders [54] or triply parallel-interpenetrating herringbone sheets both of formula $[\text{Cd}_2(\text{NO}_3)_4(\text{bpethyne})_3]_\infty$ [42]. Although both reactions were carried out in a 1:2 metal:ligand ratio, different reaction products were obtained. The only difference in the reaction conditions is the choice of alcoholic solvent. The ladders were grown from a MeOH/ CH_2Cl_2 solvent combination [54] and the herringbone grids from EtOH/ CH_2Cl_2 [42]. Although no solvent is included in either structure it is conceivable that a subtle templating effect is being observed allowing the generation of the different structures. The effect of alcoholic solvents is discussed further below. The complex $[\text{Cd}_2(\text{NO}_3)_4(\text{azpy})_3]_\infty$ [42,43] has also been structurally characterised confirming that, like its Co(II) analogue, a herringbone pattern is adopted by the 2D sheet. These sheets are triply interpenetrated in a parallel fashion as are the similar herringbone (6,3) nets observed for $[\text{Cd}_2(\text{NO}_3)_4(\text{bppent})_3]_\infty$ [$\text{bppent} = 1,5\text{-bis}(4\text{-pyridyl})\text{pentane}$] [26].

Reactions between b3ptz [24] or bptz [55] and $\text{Cd}(\text{NO}_3)_2$ have been shown to be dependent on the nature of the alcoholic solvent used. When $\text{Cd}(\text{NO}_3)_2$ is reacted with b3ptz [24] in a MeOH/ CH_2Cl_2 solution a 1:1 ligand:metal complex, $[\text{Cd}(\text{NO}_3)_2(\text{b3ptz})(\text{MeOH})_2]_\infty$, is isolated even when using 1:1, 3:2 or 2:1 ligand:metal reaction stoichiometries. This complex forms a zig-zag 1D polymer in which the Cd(II) centre does not adopt a T-shaped geometry, see Section 2.1. Replacing MeOH with EtOH results in the formation of the more familiar molecular ladder structure, Scheme 4a, $[\text{Cd}_2(\text{NO}_3)_4(\text{b3ptz})_3]_\infty$. The same ladder motif is observed when the alcoholic solvent used is $i\text{-PrOH}$ except that the clathrated EtOH molecules are replaced by CH_2Cl_2 guest molecules. In neither case is interpenetration of ladders observed.

Solvent dependence is also observed when the analogous reactions with bptz [55] are performed. As with b3ptz, [24] when the less coordinating EtOH or $i\text{-PrOH}$ solvents are used in the crystallisation process, non-interpenetrating

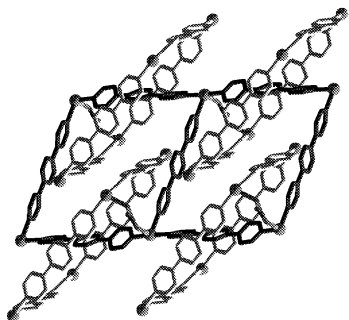


Fig. 18. View of the polyknot architecture observed for $\{[\text{Cd}_2(\text{bptz})_3(\mu\text{-NO}_3)(\text{NO}_3)_2(\text{MeOH})](\text{OH})\}_\infty$ in which nitrate bridging leads to the formation of a 3D self-penetrating structure [55].

ladders are formed. However, when crystals are grown from a MeOH/CH₂Cl₂ solution an entirely different product is isolated.

The initial structure of the complex, $\{[\text{Cd}_2(\text{bptz})_3(\mu\text{-NO}_3)(\text{NO}_3)_2(\text{MeOH})](\text{OH})\}_\infty$ [55], can be superficially regarded as a molecular ladder motif. Each Cd(II) centre is coordinated by three pyridyl N-donors which are arranged in an approximate T-shaped geometry, a monodentate nitrate, a MeOH and a bridging nitrate. Large cavities are created within each square of the ladder, which are filled by further ladders that perpendicularly interpenetrate the initial ladder. In this case, a total of two ladders are catenated through each square of any given ladder. However, each of the Cd(II) centres at the intersections of the ladder is bridged to one other Cd(II) centre by a coordinated NO₃[−] anion. This second Cd(II) is located at the corner of a square section of a perpendicularly interpenetrated ladder. As a consequence of the bridging NO₃[−] anion, all the ladders are linked together resulting in the formation of a 3D polymer where the total architecture is constructed of one molecule (Fig. 18). As this single polymeric network also exhibits polycatenation this coordination polymer can be thought of as a fused polymeric knot [55].

3.3. Summary of observed architectures with T-shaped $\text{M}(\text{NO}_3)_2$ connecting nodes

The range of compounds that give rise to a given structural motif are summarised in Table 1. It is clear from this table that T-shaped connecting nodes, although quite readily formed, act in a diversity of ways to give a variety of architectures. It is particularly noticeable that for a given $\text{M}(\text{NO}_3)_2$ salt and a given bipyridyl ligand a variety of structures have been observed. It is also of note that identical structures, and isostructural materials, can be formed for a range of $\text{M}(\text{NO}_3)_2$ salts with a given ligand with simple replacement of the metal centre within the extended lattice. This is particularly noticeable for 4,4'-bipy, the most widely studied bridging bipyridyl ligand, which forms the bilayer structure for four different $\text{M}(\text{NO}_3)_2$ salts ($\text{M} = \text{Co}, \text{Ni}, \text{Zn}, \text{Cd}$).

Of the five basic types of polymeric architecture that have been observed for $\text{M}(\text{NO}_3)_2$ nodes with bipyridyl ligands, the most common are the ladder structure and the brick-wall/herringbone 2D sheets. The incisive work of Ciani et al. [42] into the $\{[\text{M}_2(\text{NO}_3)_4[1,2\text{-bis}(4\text{-pyridyl})\text{ethyne}]]_3\}_\infty$ ($\text{M} = \text{Co}, \text{Zn}$) confirms the complexity of these systems showing that more than polymer type can be prepared from the same reaction mixture. Although some unusual structures have been prepared from tris-pyridyl $\text{M}(\text{NO}_3)_2$ networks, e.g. the $\{[\text{Cd}_2(\text{bptz})_3(\mu\text{-NO}_3)(\text{NO}_3)_2(\text{MeOH})](\text{OH})\}_\infty$ polyknot [55] and the 3D architecture adopted by one form of $[\text{Co}_2(\text{NO}_3)_4(4,4'\text{-bipy})_3]_\infty$ [34], it also seems apparent that with more careful investigations particularly of solvent/templating effects yet more architectures await discovery.

4. $\text{M}(\text{NO}_3)_2$ tetrakis-pyridyl structures

Tetrakis-pyridyl $\text{M}(\text{NO}_3)_2$ systems adopt surprisingly few different architectures with only three major types. Of these, the dominant form is the (4,4)-grid network in which the bridging bipyridyl ligands occupy equatorial coordination sites of the metal centre allowing the propagation of a 2D sheet structure. These sheets can either accommodate guest molecules within their cavities, or alternatively, the structures can interpenetrate. For the systems studied thus far the latter is significantly less common but this may be a reflection of the goals of the research groups rather than the particular systems being studied. The other two types of architecture that have been observed are double-bridged 1D chain systems and 3D architectures built from square-planar nodes. The various structures are discussed in turn.

4.1. Tetrakis-pyridyl double-bridged 1D chain structures

If the ligand is sufficiently flexible, or angular, it is possible for two ligands from a given metal node to link to the same adjacent metal node. If this is the case, as has been seen for double-bridge/single-bridge chains for tris-pyridyl systems discussed in Section 3, then in the case of tetrakis-pyridyl systems, double-bridged chains can be prepared.

For $\text{M}(\text{NO}_3)_2$ -based systems such double-bridged chain polymers will be observed if an angular or flexible ligand adopts four equatorial coordination sites around an octahedral metal centre. This is the case for $\{[\text{Ni}(\text{bppro})_2(\text{H}_2\text{O})_2](\text{NO}_3)_2\}_\infty$ in which the nitrate anion now acts in a non-bonding fashion with the axial metal coordination sites occupied by water ligands [52].

Similar constructions are observed for $[\text{Cd}(\text{NO}_3)_2(\text{bpsmb})_2]_\infty$ [56], $[\text{M}(\text{NO}_3)_2(\text{b3pdahd})_2]_\infty$ [$\text{M} = \text{Co}, \text{Cd}$; $\text{b3pdahd} = 2,5\text{-bis}(3\text{-pyridyl})\text{-3,4-diaza-2,4-hexadiene}$] [49] (Fig. 19) and $[\text{Cd}(\text{NO}_3)_2(\text{bpmfb})_2]_\infty$ [57]. In all of these instances the apical positions of the metal nodes are occupied by monodentate nitrate ligands leading to a pseudo-octahedral coordination geometry. In the latter

Table 1
Tris-pyridyl $M(\text{NO}_3)_2$ based coordination networks

Architecture	M	Ligand	Coordination framework	References
Ladder	Co	4,4'-bipy	$[\text{Co}_2(\text{NO}_3)_4(4,4'\text{-bipy})_3]_\infty$	[36]
	Co	bpeth	$[\text{Co}_2(\text{NO}_3)_4(\text{bpeth})_3]_\infty$	[37]
	Co	bpdahd	$[\text{Co}_2(\text{NO}_3)_4(\text{bpdahd})_3]_\infty$	[38]
	Co	bpethene	$[\text{Co}_2(\text{NO}_3)_4(\text{bpethene})_3]_\infty$	[40]
	Co	bpethyne	$[\text{Co}_2(\text{NO}_3)_4(\text{bpethyne})_3]_\infty$	[41,42]
	Zn	4,4'-bipy	$[\text{Zn}_2(\text{NO}_3)_4(4,4'\text{-bipy})_3]_\infty$	[46]
	Zn	bpethyne	$[\text{Zn}_2(\text{NO}_3)_4(\text{bpethyne})_3]_\infty$	[42]
	Zn	b3ptz	$[\text{Zn}_2(\text{NO}_3)_4(\text{b3ptz})_3]_\infty$	[24]
	Cd	bpmb	$[\text{Cd}_2(\text{NO}_3)_4(\text{bpmb})_3]_\infty$	[32,48]
	Cd	bpethyne	$[\text{Cd}_2(\text{NO}_3)_4(\text{bpethyne})_3]_\infty$	[54]
	Cd	b3ptz	$[\text{Cd}_2(\text{NO}_3)_4(\text{b3ptz})_3]_\infty$	[24]
	Cd	bptz	$[\text{Cd}_2(\text{NO}_3)_4(\text{bptz})_3]_\infty$	[55]
Polyknot	Cd	bptz	$\{[\text{Cd}_2(\text{bptz})_3(\mu\text{-NO}_3)(\text{NO}_3)_2(\text{MeOH})](\text{OH})\}_\infty$	[55]
Brickwall	Co	bpethyne	$[\text{Co}_2(\text{NO}_3)_4(\text{bpethyne})_3]_\infty$	[42]
	Co	azpy	$[\text{Co}_2(\text{NO}_3)_4(\text{azpy})_3]_\infty$	[44]
	Co	bpdabd	$[\text{Co}_2(\text{NO}_3)_4(\text{bpdabd})_3]_\infty$	[38]
	Co	b3pdabd	$[\text{Co}_2(\text{NO}_3)_4(\text{b3pdabd})_3]_\infty$	[35]
	Zn	bpethyne	$[\text{Zn}_2(\text{NO}_3)_4(\text{bpethyne})_3]_\infty$	[42]
	Cd	bpmfb	$[\text{Cd}_2(\text{NO}_3)_4(\text{bpmfb})_3]_\infty$	[32]
	Cd	b3pdabd	$[\text{Cd}_2(\text{NO}_3)_4(\text{b3pdabd})_3]_\infty$	[35,49]
	Cd	bpsfb	$[\text{Cd}_2(\text{NO}_3)_4(\text{bpsfb})_3]_\infty$	[50]
	Cd	bpob	$[\text{Cd}_2(\text{NO}_3)_4(\text{bpob})_3]_\infty$	[51]
Bilayer	Co	4,4'-bipy	$[\text{Co}_2(\text{NO}_3)_4(4,4'\text{-bipy})_3]_\infty$	[12,39]
	Co	bpeth	$[\text{Co}_2(\text{NO}_3)_4(\text{bpeth})_3]_\infty$	[37]
	Ni	4,4'-bipy	$[\text{Ni}_2(\text{NO}_3)_4(4,4'\text{-bipy})_3]_\infty$	[9,12]
	Zn	4,4'-bipy	$[\text{Zn}_2(\text{NO}_3)_4(4,4'\text{-bipy})_3]_\infty$	[12]
	Cd	4,4'-bipy	$[\text{Cd}_2(\text{NO}_3)_4(4,4'\text{-bipy})_3]_\infty$	[47]
Herringbone	Co	bpethyne	$[\text{Co}_2(\text{NO}_3)_4(\text{bpethyne})_3]_\infty$	[41,42]
	Co	azpy	$[\text{Co}_2(\text{NO}_3)_4(\text{azpy})_3]_\infty$	[43]
	Cd	bppro	$[\text{Cd}_2(\text{NO}_3)_4(\text{bppro})_3]_\infty$	[52]
	Cd	bpethyne	$[\text{Cd}_2(\text{NO}_3)_4(\text{bpethyne})_3]_\infty$	[42]
	Cd	azpy	$[\text{Cd}_2(\text{NO}_3)_4(\text{azpy})_3]_\infty$	[42,43]
	Cd	bpent	$[\text{Cd}_2(\text{NO}_3)_4(\text{bpent})_3]_\infty$	[26]
3D	Co	4,4'-bipy	$[\text{Co}_2(\text{NO}_3)_4(4,4'\text{-bipy})_3]_\infty$	[34]
	Co	b3pdabd	$[\text{Co}_2(\text{NO}_3)_4(\text{b3pdabd})_3]_\infty$	[35]
Single/double	Co	bpeth	$[\text{Co}_2(\text{NO}_3)_4(\text{bpeth})_3]_\infty$	[37]
	Cd	bpeth	$[\text{Cd}_2(\text{NO}_3)_4(\text{bpeth})_3]_\infty$	[53]

case the product from the reaction is templated by the *t*-butylbenzene, methylbenzoate or cumene guest molecule and alternative guests lead to alternative tetrakis-pyridyl frameworks [57].

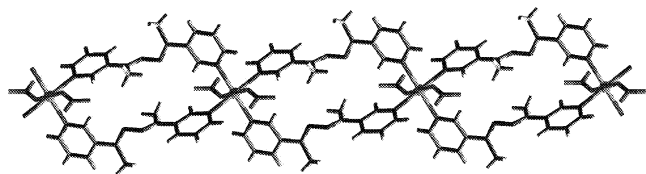
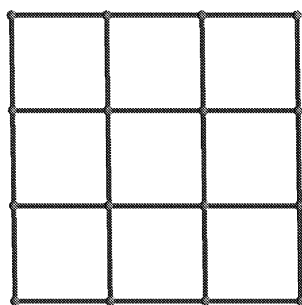


Fig. 19. View of the double-bridged chain polymer formed by $[\text{Co}(\text{NO}_3)_2(\text{b3pdabd})_2]_\infty$ utilising a tetrakis-pyridyl metal coordination mode accompanied by the angular nature of the ligand [49].

4.2. Tetrakis-pyridyl (4,4)-grid 2D frameworks

The majority of tetrakis-pyridyl coordination frameworks with $M(\text{NO}_3)_2$ nodes consist of simple 2D sheets with (4,4)-grid topology (Scheme 5). These structures use the four metal equatorial coordination positions for pyridyl coordination and the remaining axial sites are occupied by monodentate nitrate anions in most cases. It is possible for the voids within these square grids to be occupied in two ways, via guest molecules and through interpenetration. Guest inclusion is far more common than interpenetration in these systems but this may be a result of the goals of key researcher, notably Zaworotko, to inhibit interpenetration.



Scheme 5. Schematic representation of a 2D (4,4) grid structure.

4.2.1. Non-interpenetrated (4,4) 2D frameworks

Examples of (4,4)-grid networks using $M(\text{NO}_3)_2$ nodes are listed in Table 2. The most represented family of compounds are the $\{[M(\text{NO}_3)_2(4,4'\text{-bipy})_2]\cdot\text{guest}\}_\infty$ species [21,22,26,27,38,44,47,57–66]. Of these, the $\{[\text{Cd}(\text{NO}_3)_2(4,4'\text{-bipy})_2]\cdot\text{guest}\}_\infty$ group are particularly noteworthy as the only tris-pyridyl compound reported for the $\text{Cd}(\text{NO}_3)_2/4,4'\text{-bipy}$ system is a single bilayer structure [47], Section 3.2.4, and this contrasts with other $M(\text{NO}_3)_2/4,4'\text{-bipy}$ families for which many tris-products have been observed, Section 3.2. It is clear that the inclusion of guest molecules is particularly favourable in these (4,4) grid structures but in some cases selective inclusion has been demonstrated. In particular, $[\text{Cd}(\text{NO}_3)_2(4,4'\text{-bipy})_2]_\infty$ crystallises in the presence of *o*-dibromobenzene but not with the analogous *meta* or *para* isomers [58]. It has also been demonstrated that the guest can have a significant influence on the network structure for the $\{[\text{Cd}(\text{NO}_3)_2(1,4\text{-bis}[(4\text{-pyridyl)methyl]-2,3,4,5\text{-tetrafluorobenzene})_2])\}_\infty$ family of compounds [57] with either 1D chain polymers (Section 4.1), 3D (Section 4.3) or 2D (4,4) grids structures being formed, (see Table 2 for the guest molecules which template the square-grid structures). Ligands, other than 4,4'-bipy, also form (4,4) grid structures with $\text{Cd}(\text{NO}_3)_2$ of the general formula $[\text{Cd}(\text{NO}_3)_2\text{L}_2]_\infty$ and these are listed in Table 2.

The trend to form (4,4) grid structures of the formula $\{[M(\text{NO}_3)_2(4,4'\text{-bipy})_2]\cdot\text{guest}\}_\infty$ is repeated with other $M(\text{NO}_3)_2$ species and amongst these particularly notable work has been carried out by Zaworokto [63–65]. In particular it has been demonstrated that tetrakis-pyridyl $M(\text{NO}_3)_2$ grids can interpenetrate with non-covalent extended structures such as the (6,3) net formed by pyrene (Fig. 20) [65], or naphthalene [63] in which the guest molecules are associated into a supramolecular network via edge-to-face aromatic interactions.

It has been demonstrated that frameworks with large channels (ca. 15×15 Å) can be prepared by using either 1,4-bis(4-pyridyl)benzene (bpbh) or bpanth in reactions with $\text{Cu}(\text{NO}_3)_2$ or $\text{Ni}(\text{NO}_3)_2$ [22]. In some instances the cavities within a given sheet align with those in adjacent sheets to form continuous channels through the grids. These channels are then able to host columns of guest molecules. The ligand bpanth reacts with $M(\text{NO}_3)_2$ ($M=\text{Cu}, \text{Ni}$), to

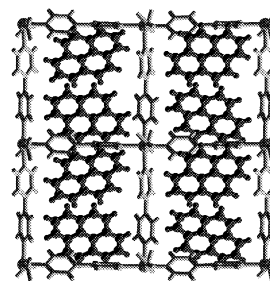


Fig. 20. View of the accommodation of pyrene in the 2D (4,4) grid structure formed by $[\text{Ni}(\text{NO}_3)_2(4,4'\text{-bipy})_2]_\infty$ [65].

afford (4,4) grid structures, $[M(\text{NO}_3)_2(\text{bpanth})_2]_\infty$ only in the presence of electron-deficient guest molecules such as nitrobenzene or benzonitrile. In contrast, if benzene is used to template the structure one of two different 1D polymers are formed with $\text{Cu}(\text{NO}_3)_2$ (section 2.1.1) or an interpenetrated square-grid type structure is formed with $\text{Ni}(\text{NO}_3)_2$ (see Section 4.2.2) [22].

It has also been demonstrated that rectangular grid structures can be prepared using $\text{Ni}(\text{NO}_3)_2$ nodes [66]. The reaction of two different ligands with $\text{Ni}(\text{NO}_3)_2$ in the presence of a benzene guest molecule affords 2D grid structures of (4,4) topology but, in this instance, each $\text{Ni}(\text{II})$ cation is bound by two different types of pyridyl ligands. Three different rectangular grid networks have been reported; $[\text{Ni}(\text{NO}_3)_2(4,4'\text{-bipy})(\text{bpbh})]_\infty$, $[\text{Ni}(\text{NO}_3)_2(\text{bpbh})(\text{bpbp})]_\infty$ (Fig. 21) and $\{[\text{Ni}(\text{NO}_3)(\text{H}_2\text{O})(\text{bpbp})(\text{bpanth})](\text{NO}_3)\}_\infty$ all in high yields (ca. 60–70%) [bpbp = 4,4'-bis(4-pyridyl)biphenyl].

4.2.2. Interpenetrated (4,4) 2D frameworks

The two methods of space filling adopted in coordination frameworks are via the incorporation of guest molecules or via interpenetration. It can be seen from the range of compounds in Table 2 that guest incorporation is common for (4,4) grid structures prepared using $M(\text{NO}_3)_2$ nodes. The second method of space filling, interpenetration, has been observed less regularly for these particular systems but some examples are known and are shown in Table 3. Interpenetration of 2D sheets can take two forms, perpendicular or parallel interpenetration [1]. Whereas perpendicular interpenetration leads to the formation of a 3D

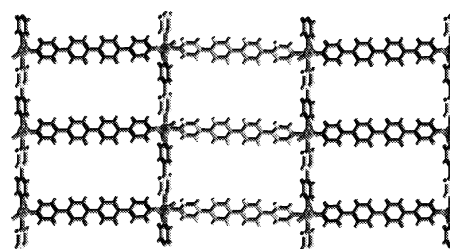


Fig. 21. View of the 2D rectangular grid structure formed by $[\text{Ni}(\text{NO}_3)_2(\text{bpbh})(\text{bpbp})]_\infty$ [66].

Table 2
Non-interpenetrating tetrakis-pyridyl $M(\text{NO}_3)_2$ based coordination networks

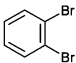
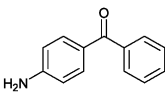
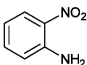
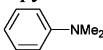
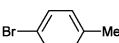
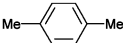
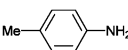
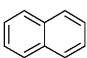
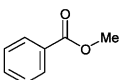
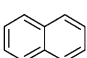
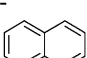
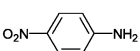
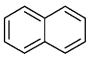
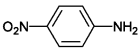
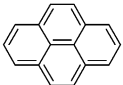
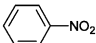
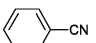
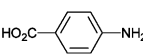
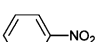
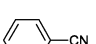
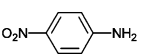
Metal	Ligand	Coordination Framework	Guest	Reference
Cd	4,4'-bipy	$[\text{Cd}(\text{NO}_3)_2(4,4'\text{-bipy})_2]_\infty$		58
Cd	4,4'-bipy	$\{[\text{Cd}(\text{H}_2\text{O})_2(4,4'\text{-bipy})_2](\text{NO}_3)_2\}_\infty$	H_2O	47,
Cd	4,4'-bipy	$\{[\text{Cd}(\text{H}_2\text{O})(\text{NO}_3)(4,4'\text{-bipy})_2](\text{NO}_3)\}_\infty$		61 59
Cd	4,4'-bipy	$[\text{Cd}(\text{NO}_3)_2(4,4'\text{-bipy})_2]_\infty$		60
Cd	bppro	$\{[\text{Cd}(\text{H}_2\text{O})_2(\text{bppro})_2](\text{NO}_3)_2\}_\infty$	H_2O	59
Cd	bpmeth	$[\text{Cd}(\text{NO}_3)_2(\text{bpmeth})_2]_\infty$	-	26
Cd	azpy	$[\text{Cd}(\text{NO}_3)_2(\text{azpy})_2]_\infty$	azpy	44
Cd	bpmfb	$[\text{Cd}(\text{NO}_3)_2(\text{bpmfb})_2]_\infty$		57
Cd	bpmfb	$[\text{Cd}(\text{NO}_3)_2(\text{bpmfb})_2]_\infty$		57
Cd	bpmfb	$[\text{Cd}(\text{NO}_3)_2(\text{bpmfb})_2]_\infty$		57
Cd	bpmfb	$[\text{Cd}(\text{NO}_3)_2(\text{bpmfb})_2]_\infty$		57
Cd	bpmfb	$[\text{Cd}(\text{NO}_3)_2(\text{bpmfb})_2]_\infty$		57
Cd	bpmfbp	$[\text{Cd}(\text{NO}_3)_2(\text{bpmfbp})_2]_\infty$		57
Cd	bpmfnap	$[\text{Cd}(\text{NO}_3)_2(\text{bpmfnap})_2]_\infty$		57
Cd	2,4'-bpma	$[\text{Cd}(\text{NO}_3)_2(2,4'\text{-bpma})_2]_\infty$	-	62
Co	4,4'-bipy	$[\text{Co}(\text{NO}_3)_2(4,4'\text{-bipy})_2]_\infty$		63
Co	4,4'-bipy	$[\text{Co}(\text{NO}_3)_2(4,4'\text{-bipy})_2]_\infty$		64
Co	b3pethyne	$\{[\text{Co}(\text{H}_2\text{O})_2(\text{b3pethyne})_2](\text{NO}_3)_2\}_\infty$	MeOH	27
Co	bpdahd	$[\text{Co}(\text{NO}_3)_2(\text{bpdahd})_2]_\infty$	C_6H_6	38
Co	bpmon	$[\text{Co}(\text{NO}_3)_2(\text{bpmon})_2]_\infty$	CH_2Cl_2	21
Ni	4,4'-bipy	$[\text{Ni}(\text{NO}_3)_2(4,4'\text{-bipy})_2]_\infty$		63
Ni	4,4'-bipy	$[\text{Ni}(\text{NO}_3)_2(4,4'\text{-bipy})_2]_\infty$		64
Ni	4,4'-bipy	$[\text{Ni}(\text{NO}_3)_2(4,4'\text{-bipy})_2]_\infty$		65

Table 2 (Continued)

Metal	Ligand	Coordination Framework	Guest	Reference
Ni	bp ^{ph}	$\{[\text{Ni}(\text{H}_2\text{O})_2(\text{bp}^{\text{ph}})](\text{NO}_3)_2\}_\infty$	MeOH, C ₆ H ₆	22
Ni	bp ^{anth}	$[\text{Ni}(\text{NO}_3)_2(\text{bp}^{\text{anth}})_2]_\infty$		22
Ni	bp ^{anth}	$[\text{Ni}(\text{NO}_3)_2(\text{bp}^{\text{anth}})_2]_\infty$		22
Ni	4,4'-bipy/ bp ^{ph}	$[\text{Ni}(\text{NO}_3)_2(4,4'\text{-bipy})(\text{bp}^{\text{ph}})]_\infty$	C ₆ H ₆	66
Ni	bp ^{ph} /bp ^{bp}	$[\text{Ni}(\text{NO}_3)_2(\text{bp}^{\text{ph}})(\text{bp}^{\text{bp}})]_\infty$	C ₆ H ₆	66
Ni	bp ^{bp} / bp ^{anth}	$\{[\text{Ni}(\text{H}_2\text{O})(\text{NO}_3)(\text{bp}^{\text{bp}})(\text{bp}^{\text{anth}})](\text{NO}_3)\}_\infty$	C ₆ H ₆	66
Cu	4,4'-bipy	$[\text{Cu}(\text{NO}_3)_2(4,4'\text{-bipy})_2]_\infty$		61
Cu	bp ^{anth}	$[\text{Cu}(\text{NO}_3)_2(\text{bp}^{\text{anth}})_2]_\infty$		22
Cu	bp ^{anth}	$[\text{Cu}(\text{NO}_3)_2(\text{bp}^{\text{anth}})_2]_\infty$		22
Zn	4,4'-bipy	$[\text{Zn}(\text{NO}_3)_2(4,4'\text{-bipy})_2]_\infty$		64

supermolecule, parallel interpenetration leads to the formation of a 2D supermolecule. Perpendicular interpenetration is more common for 2D sheet structures as parallel interpenetration requires the 2D sheet to undulate thus demanding an additional structural feature from the coordination network.

Therefore, for parallel interpenetration of (4,4) grids to be observed the 2D network has to undulate. This undulation must be generated either at the metal centre or via the ligand. The former is unlikely in a $\text{M}(\text{NO}_3)_2$ -tetrakis-pyridyl based system in which the four pyridyl ligands occupy equatorial sites of a distorted octahedral metal environment. Undulation can be generated via the ligand if the ligand is sufficiently flexible and this is the case in the compound $[\text{Cd}_2(\text{NO}_3)_4(\text{H}_2\text{O})(\text{bpro})_4]_\infty$ (Fig. 22) [26]. In contrast, the longer and potentially highly flexible ligand bp^{hex} [1,6-bis(4-pyridyl)hexane] reacts with $\text{Cd}(\text{NO}_3)_2$ to afford a near-planar (4,4) grid structure which does not undulate and interpenetrates in a perpendicular fashion such that three perpendicular $[\text{Cd}(\text{NO}_3)_2(\text{bp}^{\text{hex}})_2]_\infty$ sheets pass through each four-membered $[\text{Cd}_4(\text{bp}^{\text{hex}})_4]$ ring within a given sheet (Fig. 23) [26].

Perpendicularly interpenetrated (4,4) grid structures are also observed for $\{\text{Ni}(\text{NO}_3)_2(\text{bpdabd})_2\}_\infty$ [38], $[\text{M}(\text{NO}_3)_2(\text{bpbdyine})_2]_\infty$ (M = Cu, Co) [25] and $[\text{Ni}(\text{NO}_3)_2(\text{bp}^{\text{anth}})_2]_\infty$ [22] when prepared using a benzene template which contrasts with the non-interpenetrated forms of this compound which are formed in the presence of electron deficient guests (see Section 4.2.1). In all of these instances of perpendicular interpenetration it is notable that the bridging bipyridyl ligands used are rigid which leads to a near-planar (4,4) grid structures.

4.2.3. Other 2D tetrakis-pyridyl frameworks

One example of a 2D coordination framework which does not adopt the (4,4) grid structure but does incorporate tetrakis-pyridyl $\text{M}(\text{NO}_3)_2$ nodes has been reported [67]. $[\text{Cd}(\text{NO}_3)_2(\text{bp}^{\text{eb}})_2]_\infty$ [bp^{eb} = 1,2-bis[2-(4-pyridyl)ethyl] benzene] contains two different Cd(II) centres, one of which adopts a distorted octahedral geometry with four equatorially coordinated pyridyl groups and axially coordinated monodentate nitrate anions. The other Cd(II) cation is also coordinated by four pyridyl donors but, in this case, these N-donors occupy two axial sites and two equatorial sites

Table 3
Interpenetrating tetrakis-pyridyl $\text{M}(\text{NO}_3)_2$ based coordination networks

M	Ligand	Mode of interpenetration	Coordination framework	References
Cd	bp ^{pro}	Parallel	$[\text{Cd}_2(\text{NO}_3)_4(\text{H}_2\text{O})(\text{bp}^{\text{pro}})_4]_\infty$	[26]
Cd	bp ^{hex}	Perpendicular	$[\text{Cd}(\text{NO}_3)_2(\text{bp}^{\text{hex}})_2]_\infty$	[26]
Co	bp ^{dyine}	Perpendicular	$[\text{Co}(\text{NO}_3)_2(\text{bp}^{\text{dyine}})_2]_\infty$	[25]
Ni	bp ^{dabd}	Perpendicular	$[\text{Ni}(\text{NO}_3)_2(\text{bp}^{\text{dabd}})_2]_\infty$	[38]
Cu	bp ^{bdyine}	Perpendicular	$[\text{Cu}(\text{NO}_3)_2(\text{bp}^{\text{bdyine}})_2]_\infty$	[25]

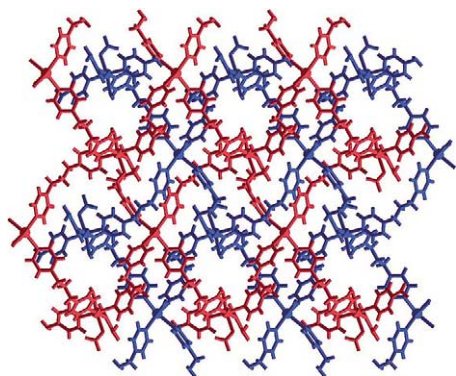


Fig. 22. View of parallel, double interpenetration in $[\text{Cd}_2(\text{NO}_3)_4(\text{H}_2\text{O})(\text{bppro})_4]_\infty$. Parallel interpenetration is allowed by the flexibility of the bppro ligand [26].

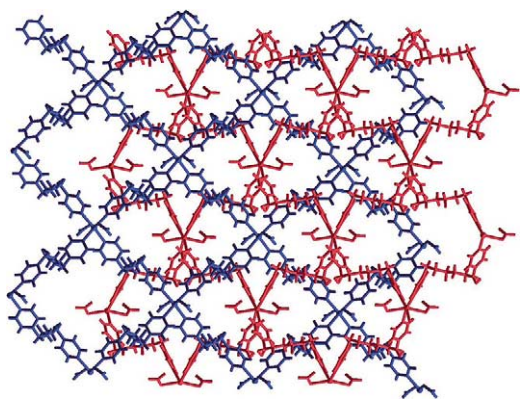


Fig. 23. View of perpendicular interpenetration observed in $[\text{Cd}(\text{NO}_3)_2(\text{bphe})_2]_\infty$. The near-planar (4,4) grid structure does not undulate despite the potentially flexible nature of the bphe ligand thus inhibiting parallel interpenetration [26].

of a pentagonal–bipyramid. The bpeb ligands bridge Cd(II) cations to form a 2D sheet which forms three distinct types of ring with either two, four or six Cd(II) nodes. This leads to the generation of a sheet with an unusual binodal $(2.4.6)(4^2.6^2)$ topology as shown in Fig. 24.

4.3. Tetrakis-pyridyl 3D architectures

Although the most common method of linking square-planar nodes generates 2D grid structures, Section 4.2, it is also possible to generate 3D architectures from such nodes simply by rotating the planes described by adjacent metal nodes. The most common 3D structure generated from square-planar nodes adopts the $\text{Cd}(\text{SO}_4)$ topology, Scheme 6, though others are possible. While 3D architec-

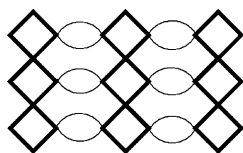
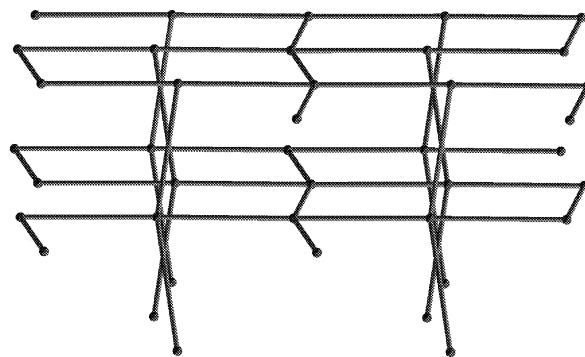


Fig. 24. Schematic representation of the unusual binodal $(2.4.6)(4^2.6^2)$ topology exhibited by $[\text{Cd}(\text{NO}_3)_2(\text{bpeb})_2]_\infty$ [67].



Scheme 6. Schematic representation of the 3D $\text{Cd}(\text{SO}_4)$ topology.

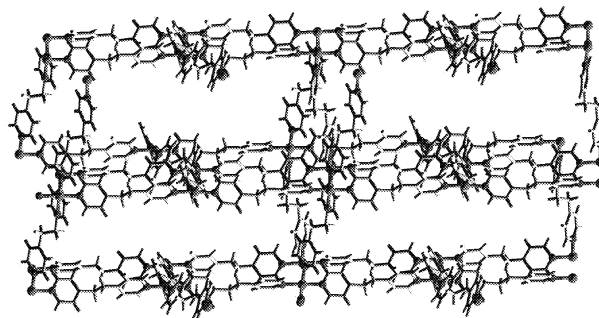


Fig. 25. View of the $\text{Cd}(\text{SO}_4)$ -type 3D architecture, $[\text{Cu}(\text{NO}_3)_2(\text{bpeth})_2]_\infty$, formed using tetrakis-pyridyl $\text{M}(\text{NO}_3)_2$ connecting nodes [18].

tures are rare for tetrakis-pyridyl $\text{M}(\text{NO}_3)_2$ coordination frameworks, two examples of $\text{Cd}(\text{SO}_4)$ -type structures have been reported, $[\text{Cu}(\text{NO}_3)_2(\text{bpeth})_2]_\infty$ [18] (Fig. 25) and $[\text{Cu}(\text{NO}_3)_2(\text{bphe})_2]_\infty$ [68]. In the case of $[\text{Cu}(\text{NO}_3)_2(\text{bpeth})_2]_\infty$, the Cu(II) centre adopts a significantly Jahn-Teller distorted coordination environment with four equatorially bound pyridyl donors and significantly elongated $\text{Cu} \cdots \text{O}$ interactions [$\text{Cu}-\text{O} = 2.366(4), 2.486(4) \text{ \AA}$] in the axial sites. Although this structure was originally described as adopting an NbO topology [18] it was later confirmed as actually adopting a $\text{Cd}(\text{SO}_4)$ arrangement [31]. Whereas $[\text{Cu}(\text{NO}_3)_2(\text{bpeth})_2]_\infty$ exhibits twofold interpenetration, the longer ligand in $[\text{Cu}(\text{NO}_3)_2(\text{bphe})_2]_\infty$ [68] leads to a higher fourfold interpenetration as would be expected for the longer bridging ligand [17].

A more complex 3D architecture has also been observed for a $\text{Cu}(\text{NO}_3)_2$ -based structure with square-planar nodes. $[\text{Cu}(\text{NO}_3)_2(\text{bpethyne})_2]_\infty$ [31] adopts a structure with $7^5.9$ topology (Fig. 26) which is unique amongst four-connected

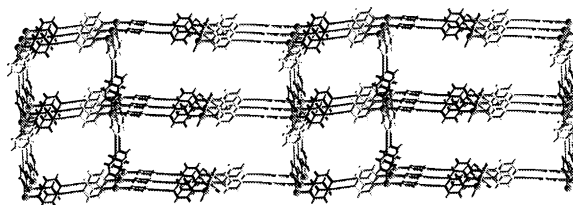


Fig. 26. View of the dense net structure formed by $[\text{Cu}(\text{NO}_3)_2(\text{bpethyne})_2]_\infty$ which adopts a $7^5.9$ topology [31].

nets in that it exhibits no shortest circuits smaller than heptagons and also has the highest topological density of any four-connected net [69]. This framework exhibits threefold interpenetration but, in this instance, the three nets are topologically but not chemically equivalent. All three frameworks adopt Cu(II) coordination environments which have four equatorial pyridyl donors but the axial, substituents differ between the nets. In one net both axial sites are occupied by two loosely bound water molecules but, in the other two nets one site is occupied by a water ligand and one by a monodentate nitrate anion.

More recently, diamondoid networks have been reported for the framework $[\text{Cd}(\text{NO}_3)_2(\text{bpmfb})_2]_\infty$ [57]. This is surprising as diamond frameworks are usually constructed using tetrahedral metal nodes rather than metal centres with higher coordination environments [15,17]. In this instance, the flexibility of the Cd(II) coordination environment coupled with the flexibility of the bpmfb ligand allows the formation of this diamondoid arrangement. This framework is produced in the presence of particular guest molecules such as phenyl acetate whereas, other guest molecules afford either 1D or 2D networks which also contain tetrakis-pyridyl metal coordination environments (see Sections 4.1 and 4.2.1).

5. Architectures containing more than one type of $\text{M}(\text{NO}_3)_2$ node

Reaction of $\text{Ni}(\text{NO}_3)_2$ with azpy in a 1:2 ratio affords a complex network structure [45]. Structural characterisation revealed two independent 2D sheets within the same lattice. In one sheet the $\text{Ni}(\text{NO}_3)_2$ units adopt the familiar T-shaped geometry and these are linked through the azpy ligands to give a brickwall type structure, Scheme 4b. However, in the other sheet the $\text{Ni}(\text{NO}_3)_2$ coordinates four pyridyl donors with the two monodentate nitrate anions coordinating the metal centre in mutually *trans* sites. This leads to the formation of a (4,4) sheet, $[\text{Ni}(\text{NO}_3)_2(\text{azpy})_2]_\infty$, which interpenetrates the independent (6,3) brickwall sheet, $[\text{Ni}_2(\text{NO}_3)_4(\text{azpy})_3]_\infty$, at an angle of ca. 45° to give a polycatenated 3D structure (Fig. 27). The formation of the two different $\text{Ni}(\text{NO}_3)_2$ junctions within the same compound is most unusual but the two networks that are observed are both familiar (see Sections 3 and 4).

Similarly to the $\text{Ni}(\text{NO}_3)_2/\text{azpy}$ system the reaction of $\text{Cd}(\text{NO}_3)_2$ with bbbp affords a compound which consists of three different types of coordination polymers which interpenetrate within the same crystal [70]. The first of three interlocked architectures is a 2D square-grid structure, $[\text{Cd}(\text{NO}_3)_2(\text{bbb})_2]_\infty$, constructed from distorted octahedral $\text{Cd}(\text{NO}_3)_2$ centres with axially coordinated monodentate nitrate anions and four equatorially coordinated bbbp ligands. These 2D sheets pack in a coplanar manner forming channels with dimensions of ca. $10 \times 20 \text{ \AA}$ and a large inter-layer spacing of 10.9 \AA .

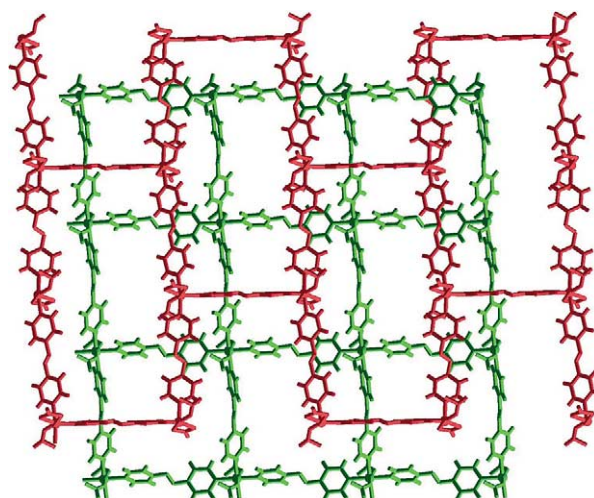


Fig. 27. View of the interpenetrating (4,4) $[\text{Ni}(\text{NO}_3)_2(\text{azpy})_2]_\infty$ and (6,3) $[\text{Ni}_2(\text{NO}_3)_4(\text{azpy})_3]_\infty$ brickwall 2D sheets observed in $\{[\text{Ni}(\text{NO}_3)_2(\text{azpy})_2][\text{Ni}_2(\text{NO}_3)_4(\text{azpy})_3]\}_\infty$ [45].

Running perpendicular to the square-grid sheets, and through the channels formed by these sheets is a double linear chain, $\{[\text{Cd}_4(\text{NO}_3)_6(\text{bbb})_4]^{2+}\}_\infty$. This 1D polymer consists of $[\text{Cd}(\text{bbb})]_\infty$ chains which are cross-linked via nitrate bridges. The remaining coordination sites on each Cd(II) centre are occupied by either nitrate anions or MeOH ligands and four crystallographically independent Cd(II) centres are observed within this double linear chain.

The final polymeric motif observed in this extremely unusual system are simple linear $\{[\text{Cd}(\text{NO}_3)_3(\text{bbb})]^- \}_\infty$ chains which run between the square-grid sheets and perpendicularly with respect to the double linear-chains. The complexity of the three architectures observed within a single structure illustrate the complexity of $\text{Cd}(\text{NO}_3)_2$ -bipyridyl-based coordination polymers [70].

Similarly, $\text{Cd}(\text{NO}_3)_2$ reacts with bpmob to afford a crystal system with two different $\text{Cd}(\text{NO}_3)_2$ coordination modes [71]. In this case the resultant architectures are much simpler than those observed in the bbbp system described above [70]. Two different 1D coordination polymers are observed within the same crystal. Firstly, a 1D chain is observed, $[\text{Cd}(\text{NO}_3)_2(\text{H}_2\text{O})(\text{trans-bpmob})]_\infty$, which includes *trans* bis-pyridyl Cd(II) centres which are also coordinated by one water ligand, one bidentate nitrate, and one bridging nitrate anion which links these chains into pairs. This is a motif observed with other nitrate-bridged 1D polymers (see Section 2). The other polymer observed in this system is also 1D but the flexible ligand adopts a *cis*-configuration such that it bridges metal centres to form tetrakis-pyridyl Cd(II) centres, $[\text{Cd}(\text{NO}_3)_2(\text{cis-bpmob})_2]_\infty$. The remaining axial coordination sites on the octahedral Cd(II) centre are accommodated by coordinated nitrate anions. These two chains are both well known for other $\text{M}(\text{NO}_3)_2/\text{ligand}$ systems but this is the only example in which both are observed within a single crystal system.

$\text{Cu}(\text{NO}_3)_2$ reacts with bphex to give another coordination polymer system in which two motifs are observed [68]. In this case, as with the bpmob system discussed above, two 1D polymers are observed which both involve propagation via the bphex ligand. One, $[\text{Cu}(\text{NO}_3)_2(\text{bphex})_3]_\infty$, adopts a simple chain arrangement but, each Cu(II) node is decorated by two pendant bphex ligands. The other coordination polymer forms a chain built from linked $[\text{Cu}(1,6\text{-bis}(4\text{-pyridyl})\text{hexane})_2]$ metallacycles with each Cu(II) adopting a tetrakis-pyridyl coordination sphere, as discussed in Section 4.1, with one monodentate nitrate anion and a single water ligand, $\{[\text{Cu}(\text{NO}_3)(\text{bphex})_2(\text{H}_2\text{O})](\text{NO}_3)\}_\infty$. The two chains are interlocked such that the first chain penetrates through the metallacycles formed by the second chain leading to a polyrotaxane structure.

6. Conclusions, structural reliability and future developments

It is clear from Sections 2–4 that $\text{M}(\text{NO}_3)_2$ nodes can adopt a range of different coordination spheres with the number of pyridyl donors ranging from two to four. This variation in the number of pyridyl donors is clearly very significant as the bridging bipyridyl ligands are predominantly responsible for polymeric propagation in these species.

The role of the nitrate anion is also clearly important in these species as the denticity and bridging vs. non-bridging ability of this anion has two key functions. Firstly, through variation in the coordination mode of the nitrate group, the rest of the coordination sphere at the metal centre is significantly affected and potentially alters the number of bipyridyl bridges linked to any metal node. Secondly, the potential of the nitrate anion to bridge metal centres is clearly important in determining framework structure and topology.

It is also apparent from the wide variety of structures seen for the same metal and ligand that a very subtle energy balance can exist between different structural motifs. Sometimes the change in structure is a result of small changes in reaction conditions or addition of a template to the crystallisation process [36]. In other instances, more than one architecture is formed from the same reaction process [41,42].

As this subtle balance exists between the different architectures formed by $\text{M}(\text{NO}_3)_2$ -bipyridyl systems, it would be difficult to consider the $\text{M}(\text{NO}_3)_2$ building-blocks as a reliable connecting node. In fact, $\text{M}(\text{NO}_3)_2$ nodes are particularly flexible and prone to external influences readily changing their connectivity or geometry leading to different products. Thus, it is difficult to anticipate the geometry of the $\text{M}(\text{NO}_3)_2$ centre from a given reaction with a bipyridyl ligand. It is, perhaps, even more difficult to predict the resulting network architecture from a given $\text{M}(\text{NO}_3)_2$ coordination environment. This is probably most noticeable for the tris-pyridyl species, see Section 3.

$\text{M}(\text{NO}_3)_2$ -based coordination polymers lead to a wide variety of structural types and some particularly fascinating

architectures and unusual forms of supramolecular isomerism [3]. Indeed, in terms of discovering new structural types and architectures, the families of $\text{M}(\text{NO}_3)_2$ structures are as varied as any other area of coordination framework chemistry. This makes studying these systems both challenging and exciting. The flexibility of the coordination frameworks with respect to guest inclusion [57] and their remarkable ability to include guest molecules, including gases [10,12], also makes these systems particularly attractive in terms of their future development as functional materials. It can be anticipated that this area of coordination frameworks will continue to expand with further remarkable structural types being discovered and being applied to the solution of current technological challenges.

Acknowledgements

We thank the EPSRC for funding (SAB).

References

- [1] S.R. Batten, R. Robson, *Angew. Chem. Int. Ed.* 37 (1998) 1460.
- [2] A.J. Blake, N.R. Champness, P. Hubberstey, W.-S. Li, M. Schröder, M.A. Withersby, *Coord. Chem. Rev.* 183 (1999) 117.
- [3] B. Moulton, M.J. Zaworotko, *Chem. Rev.* 101 (2001) 1629.
- [4] M. Fujita, *Comprehensive Supramolecular Chemistry*, Vol. 9, Pergamon Press, Oxford, 1996, p. 253.
- [5] (a) J.-M. Lehn, *Supramolecular Chemistry*, VCH, Weinheim, Germany, 1995;
(b) J.-M. Lehn, *Comprehensive Supramolecular Chemistry*, Pergamon Press, Oxford, 1996.
- [6] (a) G.R. Desiraju (Ed.), *Perspectives in Supramolecular Chemistry: The Crystal as a Supramolecular Entity*, Vol. 2, Wiley, Chichester, 1996;
(b) G.R. Desiraju, *Angew. Chem. Int. Ed. Engl.* 34 (1995) 2311;
(c) G.R. Desiraju, *The Design Of Organic Solids*, Elsevier, Amsterdam, 1989;
(d) C.B. Aakeroy, *Acta Crystallogr. B* 53 (1997) 569.
- [7] (a) D. Venkataraman, G.B. Gardner, S. Lee, J.S. Moore, *J. Am. Chem. Soc.* 117 (1995) 11600;
(b) D.M.L. Goodgame, D.A. Garchvogel, D.J. Williams, *Angew. Chem. Int. Ed. Engl.* 38 (1999) 153;
(c) B.F. Abrahams, P.A. Jackson, R. Robson, *Angew. Chem. Int. Ed. Engl.* 37 (1998) 2657.
- [8] A.J. Blake, N.R. Champness, A.N. Khlobystov, S. Parsons, M. Schröder, *Angew. Chem. Int. Ed.* 39 (2000) 2317.
- [9] C.J. Kepert, M.J. Rosseinsky, *Chem. Commun.* (1999) 375.
- [10] A.J. Fletcher, E.J. Cussen, T.J. Prior, M.J. Rosseinsky, C.J. Kepert, K.M. Thomas, *J. Am. Chem. Soc.* 123 (2001) 10001.
- [11] T.M. Reineke, M. Eddaoudi, M. Fehr, D. Kelley, O.M. Yaghi, *J. Am. Chem. Soc.* 121 (1999) 1651.
- [12] M. Kondo, T. Yoshitomi, K. Seki, H. Matsuzaka, S. Kitagawa, *Angew. Chem. Int. Ed.* 36 (1997) 1725.
- [13] H. Zhao, R.A. Heintz, X. Ouyang, K.R. Dunbar, C.F. Campana, R.D. Rogers, *Chem. Mater.* 11 (1999) 736.
- [14] W. Lin, O.R. Evans, *Acc. Chem. Res.* 35 (2002) 511.
- [15] R. Robson, B.F. Abrahams, S.R. Batten, R.W. Gable, B.F. Hoskins, J.P. Liu, *ACS Symp. Ser.* 499 (1992) 256.
- [16] A.N. Khlobystov, A.J. Blake, N.R. Champness, D.A. Lemenovskii, A.G. Majouga, N.V. Zyk, M. Schröder, *Coord. Chem. Rev.* 222 (2001) 137.

- [17] (a) A.J. Blake, N.R. Champness, S.S.M. Chung, W.-S. Li, M. Schröder, *Chem. Commun.* (1997) 1005;
(b) L.R. MacGillivray, S. Subramanian, M.J. Zaworotko, *J. Chem. Soc. Chem. Commun.* (1994) 1325.
- [18] K.N. Power, T.L. Hennigar, M.J. Zaworotko, *Chem. Commun.* (1998) 595.
- [19] M. Eddaoudi, J. Kim, M. O'Keeffe, O.M. Yaghi, *J. Am. Chem. Soc.* 124 (2002) 376.
- [20] Z. Atherton, D.M.L. Goodgame, S. Menzer, D.J. Williams, *Polyhedron* 18 (1999) 273.
- [21] S. Banfi, L. Carlucci, E. Caruso, G. Ciani, D.M. Proserpio, *J. Chem. Soc. Dalton Trans.* (2002) 2714.
- [22] K. Biradha, M. Fujita, *J. Chem. Soc. Dalton Trans.* (2000) 3805.
- [23] S.A. Barnett, A.J. Blake, N.R. Champness, J.E.B. Nicolson, C. Wilson, *J. Chem. Soc. Dalton Trans.* (2001) 567.
- [24] M.A. Withersby, A.J. Blake, N.R. Champness, P. Hubberstey, W.-S. Li, M. Schröder, *Inorg. Chem.* 38 (1999) 2259.
- [25] M.B. Zaman, M.D. Smith, H.-C. zur Loye, *Chem. Mater.* 13 (2001) 3534.
- [26] M.J. Plater, M.R.St.J. Foreman, T. Gelbrich, S.J. Coles, M.B. Hursthouse, *J. Chem. Soc. Dalton Trans.* (2000) 3065.
- [27] M.B. Zaman, M.D. Smith, D.M. Ciurtin, H.-C. zur Loye, *Inorg. Chem.* 41 (2002) 4895.
- [28] T.X. Neenan, W.L. Driessen, J.G. Haasnoot, J. Reedijk, *Inorg. Chim. Acta* 247 (1996) 43.
- [29] Z. Wang, R.-G. Xiong, E. Naggar, B.M. Foxman, W. Lin, *Inorg. Chim. Acta* 288 (1999) 215.
- [30] A.N. Khlobystov, M.T. Brett, A.J. Blake, N.R. Champness, C. Wilson, M. Schröder, *J. Am. Chem. Soc.* 125 (2003) 6753.
- [31] L. Carlucci, G. Ciani, P. Macchi, D.M. Proserpio, *Chem. Commun.* (1998) 1837.
- [32] M. Fujita, Y.J. Kwon, O. Sasaki, K. Yamaguchi, K. Ogura, *J. Am. Chem. Soc.* 117 (1995) 7287.
- [33] (a) A.F. Cameron, D.W. Taylor, R.H. Nuttall, *J. Chem. Soc. Dalton Trans.* (1972) 1603;
(b) A.F. Cameron, D.W. Taylor, R.H. Nuttall, *J. Chem. Soc. Dalton Trans.* (1972) 1609.
- [34] H. Gudbjartson, K. Biradha, K.M. Poirier, M.J. Zaworotko, *J. Am. Chem. Soc.* 121 (1999) 2599.
- [35] Y.-B. Dong, M.D. Smith, R.C. Layland, H.-C. zur Loye, *Chem. Mater.* 12 (2000) 1156.
- [36] P. Losier, M.J. Zaworotko, *Angew. Chem. Int. Ed.* 35 (1996) 2779.
- [37] T.L. Hennigar, D.C. MacQuarrie, P. Losier, R.D. Rogers, M.J. Zaworotko, *Angew. Chem. Int. Ed.* 36 (1997) 972.
- [38] D.M. Ciurtin, Y.-B. Dong, M.D. Smith, T. Barclay, H.-C. zur Loye, *Inorg. Chem.* 40 (2001) 2825.
- [39] K.N. Power, T.L. Hennigar, M.J. Zaworotko, *New J. Chem.* 22 (1998) 177.
- [40] O.-S. Jung, S.H. Park, K.M. Ki, H.G. Jang, *Inorg. Chem.* 37 (1998) 5781.
- [41] Y.-B. Dong, R.C. Layland, N.G. Pschirer, M.D. Smith, U.H.F. Bunz, H.-C. zur Loye, *Chem. Mater.* 11 (1999) 1413.
- [42] L. Carlucci, G. Ciani, D.M. Proserpio, *J. Chem. Soc. Dalton Trans.* (1999) 1799.
- [43] M.A. Withersby, A.J. Blake, N.R. Champness, P.A. Cooke, P. Hubberstey, M. Schröder, *New J. Chem.* 23 (1999) 573.
- [44] M. Kondo, M. Shimamura, S. Noro, S. Minakoshi, A. Ashami, K. Seki, S. Kitagawa, *Chem. Mater.* 12 (2000) 1288.
- [45] L. Carlucci, G. Ciani, D.M. Proserpio, *New J. Chem.* 22 (1998) 1319.
- [46] B.D. Wagner, G.J. McManus, B. Moulton, M.J. Zaworotko, *Chem. Commun.* (2002) 2176.
- [47] J.T. Sampanthar, J.J. Vittal, *Cryst. Eng.* 2 (1999) 251.
- [48] M. Fujita, O. Sasaki, K. Watanabe, K. Ogura, K. Yamaguchi, *New J. Chem.* 22 (1998) 189.
- [49] Y.-B. Dong, M.D. Smith, H.-C. zur Loye, *Inorg. Chem.* 39 (2000) 4927.
- [50] D.M.L. Goodgame, D.A. Grachvogel, S. Holland, N.J. Long, A.J.P. White, D.J. Williams, *J. Chem. Soc. Dalton Trans.* (1999) 3473.
- [51] M. Kondo, A. Asami, K. Fujimoto, S. Noro, S. Kitagawa, T. Ishii, H. Matsuzaka, *Int. J. Inorg. Mater.* 1 (1999) 73.
- [52] C.V.K. Sharma, R.J. Diaz, A.J. Hessheimer, A. Clearfield, *Cryst. Eng.* 3 (2000) 201.
- [53] M. Fujita, Y.J. Kwon, M. Miyazawa, K. Ogura, *J. Chem. Soc. Chem. Commun.* (1994) 1977.
- [54] Y.-B. Dong, R.C. Layland, M.D. Smith, N.G. Pschirer, U.H.F. Bunz, H.-C. zur Loye, *Inorg. Chem.* 11 (1999) 3056.
- [55] M.A. Withersby, A.J. Blake, N.R. Champness, P. Hubberstey, W.-S. Li, M. Schröder, *J. Am. Chem. Soc.* 122 (2000) 4044.
- [56] R. Wang, M. Hong, J. Weng, W. Su, R. Cao, *Inorg. Chem. Commun.* 3 (2000) 486.
- [57] K. Kasai, M. Aoyagi, M. Fujita, *J. Am. Chem. Soc.* 122 (2000) 2140.
- [58] M. Fujita, Y.J. Kwon, S. Washizu, K. Ogura, *J. Am. Chem. Soc.* 116 (1994) 1151.
- [59] Z.-Y. Fu, P. Lin, W.-X. Du, L. Chen, C.-P. Cui, W.-J. Zhang, X.-T. Wu, *Polyhedron* 20 (2001) 1925.
- [60] S.D. Huang, B.J. Lewandowski, C. Liu, Y. Shan, *Acta Crystallogr. Sect. C* 55 (1999) 2016.
- [61] M.-L. Tong, S.-L. Zheng, X.-M. Chen, *Polyhedron* 19 (2000) 1809.
- [62] Z. Wang, R.-G. Xiong, B.M. Foxman, S.R. Wilson, W. Lin, *Inorg. Chem.* 38 (1999) 1523.
- [63] K. Biradha, K.V. Domasevitch, C. Hogg, B. Moulton, K.N. Power, M.J. Zaworotko, *Cryst. Eng.* 2 (1999) 37.
- [64] B. Moulton, E.B. Rather, M.J. Zaworotko, *Cryst. Eng.* 4 (2001) 309.
- [65] K. Biradha, K.V. Domasevitch, B. Moulton, C. Seward, M.J. Zaworotko, *Chem. Commun.* (1999) 1327.
- [66] K. Biradha, M. Fujita, *Chem. Commun.* (2001) 15.
- [67] M.J. Plater, M.R.St.J. Foreman, J.M.S. Skakle, *Cryst. Eng.* 4 (2001) 293.
- [68] M.J. Plater, M.R.St.J. Foreman, T. Gelbrich, M.B. Hursthouse, *Cryst. Eng.* 4 (2001) 319.
- [69] M. O'Keeffe, B.G. Hyde, *Crystal Structures I: Pattern and Symmetry*, Mineralogical Society of America, Washington, DC, 1996.
- [70] K. Biradha, M. Fujita, *Chem. Commun.* (2002) 1866.
- [71] H. Hou, Y. Fan, L. Zhang, C. Du, Y. Zhu, *Inorg. Chem. Commun.* 4 (2001) 168.